SELENIUM AS PALEO-OCEANOGRAPHIC PROXY: A FIRST ASSESSMENT

A Thesis
Presented to
The Academic Faculty

By

Kristen Mitchell

In Partial Fulfillment
of the Requirements for the Degree
Master of Science in the
School of Earth and Atmospheric Science

Georgia Institute of Technology

May 2011

SELENIUM AS PALEO-OCEANOGRAPHIC PROXY: A FIRST ASSESSMENT

Approved by:

Dr. Philippe Van Cappellen
School of Earth and Atmospheric Sciences
Georgia Institute of Technology

Dr. Ellery Ingall
School of Earth and Atmospheric Sciences
Georgia Institute of Technology

Dr. Paul R. D. Mason
Faculty of Geosciences
Utrecht University

Date Approved: March 28, 2011

ACKNOWLEDGEMENTS

I thank my advisor Dr. Philippe Van Cappellen for discussions and support and keeping me moving. I would also like to thank my committee members, Dr. Paul Mason and Dr. Ellery Ingall for suggestions and discussions.

I would also like to thank Dr. Thomas Johnson for his support and guidance with analytical techniques without which this work could not have been completed.

I would like to thank those who contributed samples and their insights into the sample locations Dr. Ellery Ingall, Dr. Timothy Lyons, Dr. Benjamin Gill, Dr. Gert-Jan Reichart, Julia Diaz, and Jeremy Owens.

TABLE OF CONTENTS

LIST OF TABLES

LIST OF FIGURES

SUMMARY

Selenium (Se) is an essential trace element, which, with multiple oxidation states and six stable isotopes, has the potential to be a powerful paleo-environmental proxy. In this study, Se concentrations and isotopic compositions were analyzed in a suite of about 120 samples of fine-grained marine sedimentary rocks and sediments spanning the entire Phanerozoic. While the selenium concentrations vary greatly (0.22 to 72 ppm), the $\delta^{82/76}$Se values fall in a fairly narrow range from -1 to +1‰, with the exception of laminated black shales from the New Albany Shale formation (Devonian), which have $\delta^{82/76}$Se values of up to +2.20‰. Black Sea sediments (Holocene) and sedimentary rocks from the Alum Shale formation (Late Cambrian) have Se/TOC ratios and $\delta^{82/76}$Se values close to those found in modern marine plankton ($1.72 \times 10^{-6} \pm 1.55 \times 10^{-7}$ mol/mol and 0.42±0.22‰). (Note: TOC = total organic carbon.) For the other sedimentary sequences, the Se/TOC ratios indicate enrichment in selenium relative to marine plankton. Additional input of isotopically light terrigenous Se ($\delta^{82/76}$Se ≈ -0.42‰) may explain the Se data measured in recent Arabian Sea sediments (Pleistocene). The very high Se concentrations in sedimentary sequences that include the Cenomanian-Turonian Ocean Anoxic Event (OAE) 2 possibly reflect a significantly enhanced input of volcanogenic Se to the oceans. As the latter has an isotopic composition ($\delta^{82/76}$Se ≈ 0‰) not greatly different from marine plankton, the volcanogenic source does not impart a distinct signature to the sedimentary Se isotope record. The lowest $\delta^{82/76}$Se values are observed in the OAE2 samples from Demerara Rise and Cape Verde Basin cores ($\delta^{82/76}$Se = -0.95 to 1.16‰) and are likely due to fractionation associated with microbial or chemical reduction of Se oxyanions in the euxinic water column. In contrast, a limiting availability of seawater Se during periods of increased organic matter burial is thought to be responsible for the elevated $\delta^{82/76}$Se values and low Se/TOC ratios in the black shales of the New Albany Shale formation. Overall, our results suggest that Se data may provide useful information on paleodepositional conditions, when included in a multi-proxy approach.

CHAPTER 1. INTRODUCTION

Selenium (Se) exhibits four major oxidation states in the environment: -II, 0, +IV, and +VI. It also has six stable isotopes: ^{74}Se, ^{76}Se, ^{77}Se, ^{78}Se, ^{80}Se, and ^{82}Se. Given the multiple oxidation states and multiple isotopes, selenium has the potential to be a powerful paleoenvironmental proxy. Here, we evaluate whether selenium isotope signatures in marine shales and mudstones can yield information on the paleoredox conditions in the overlying water column. Fine grained sedimentary rocks are selected because they contain relatively high Se concentrations (Turekian, 1961).

Selenium concentrations in seawater are very low (<1 μM or <0.08 ppm, Cutter and Bruland, 1984). Dissolved selenium in the water column exists as selenate and selenite oxyanions, and as dissolved organic selenium (Baines, 2001; Cutter and Bruland, 1984). Selenate and selenite exhibit nutrient-like depth distributions in the ocean (Cutter and Bruland, 1984; Cutter and Cutter, 1995; Johnson, 2004; Measures and Burton, 1980a, b; Measures et al., 1983). At oxygen concentrations below 10 μM, the dominant form of dissolved selenium is organic selenide, with selenate and selenite often at or below detection (Cutter, 1982). The presence of organic selenide in deep reducing waters is likely due to stabilization of organic selenide formed produced by organic matter degradation (Rue et al., 1997).

Assimilatory uptake by plankton accounts for most of the dissolved selenium removal in the surface ocean (Cutter and Bruland, 1984). Selenium is generally taken up as selenite or selenate during assimilatory reduction, although dissolved organic selenide can also be directly assimilated from seawater (Baines, 2001). The major supply of selenium to marine sediments appears to be the deposition of organic detritus at the seafloor (Baines and Fisher, 2001; Cutter and Bruland, 1984; Ohlendorf, 1989; Wrench and Measures, 1982). The present-day deposition flux of selenium is estimated to range from 7.4×10^9 to 1×10^{10} g Se/year (Wrench and Measures, 1982).

Selenium oxyanions can be reduced via dissimilatory reduction mechanisms, which are carried out by a number of different microbes (Herbel et al., 2003; Oremland, 1991, 1994; Oremland et al., 1994; Oremland et al., 1989; Oremland et al., 1990). Dissimilatory reduction generally only occurs in the absence of molecular oxygen. Microorganisms capable of growth with selenium (IV, VI) as terminal

electron acceptor can be placed in four groups, based on growth conditions and phylogeny: hyperthermophilic archaea, thermophilic bacteria, mesophilic gram-negative bacteria, and γ-, δ- and ε-proteobacteria (J.S. Geelhoed, personal communication, 2007). The majority of the currently described species utilize organic electron donors in the form of short organic acids, alcohols or sugars. The predominant end-product of dissimilatory reduction of selenium oxyanions is red elemental selenium (Herbel et al., 2003; Oremland, 1991, 1994; Oremland et al., 1994; Oremland et al., 1989; Oremland et al., 1990). In laboratory experiments, the latter is usually identified by the appearance of a characteristic red color.

Selenate and selenite oxyanions sorb to organic matter, iron oxides and iron sulfides (Balistrieri and Chao, 1987; Bruggeman et al., 2005; Scheinost and Charlet, 2008). Selenite, however, tends to bind more strongly than selenate. For instance, selenite has been shown to form strong inner-sphere complexes at the surface of α-FeOOH (goethite), while selenate only forms weak outer-sphere complexes (Hayes et al., 1987). The adsorption of Se(VI) and Se(IV) oxyanions on goethite depends on the presence of competing anions, in particular phosphate and organic acids (Balistrieri and Chao, 1987). The pH also plays a major role, with the strongest adsorption of Se(IV) and Se(VI) at low pH. Selenium oxyanions become more mobile with increasing alkalinity, with essentially no adsorption above pH 11 (Howard III, 1977; Neal et al., 1987). Adsorption of Se on iron oxides imparts only small isotopic fractionations (ε=0.8‰ Johnson and Bullen, 2004; Johnson et al., 1999).

Adsorption of selenite on pyrite (FeS_2) results in the subsequent reduction to elemental selenium (Bruggeman et al., 2005). Selenite also adsorbs to mackinawite (FeS) and, depending on pH, is reduced to either elemental selenium or Se(-II) in the form of FeSe (Scheinost and Charlet, 2008). Adsorption of selenite to siderite causes only minimal reduction to elemental selenium, with most of the selenite remaining adsorbed. In the presence of magnetite, formation of an unidentified mixed-valence (Fe(II)-Fe(III)) iron selenide has been observed (Scheinost and Charlet, 2008). Thus, several abiotic pathways may lead to burial in marine sediments of selenium under the form of adsorbed selenite, elemental selenium or iron-bound selenide.

The stable isotopes of selenium can be fractionated during redox transformations. The redox pathways that have been shown to produce significant selenium isotope fractionation include dissimilatory microbial reduction and abiotic reduction by green rust of Se(VI) and Se(IV) oxyanions (Ellis et al., 2003; Herbel et al., 2000; Johnson and Bullen, 2003, 2004). Large isotope fractionations have also been observed in chemical reduction experiments performed under highly acidic conditions and at high temperatures (Krouse and Thode, 1962; Rashid and Krouse, 1985; Rees and Thode, 1966). Isotope fractionations associated with selenite adsorption and subsequent abiotic reduction under near-surface conditions have yet to be investigated.

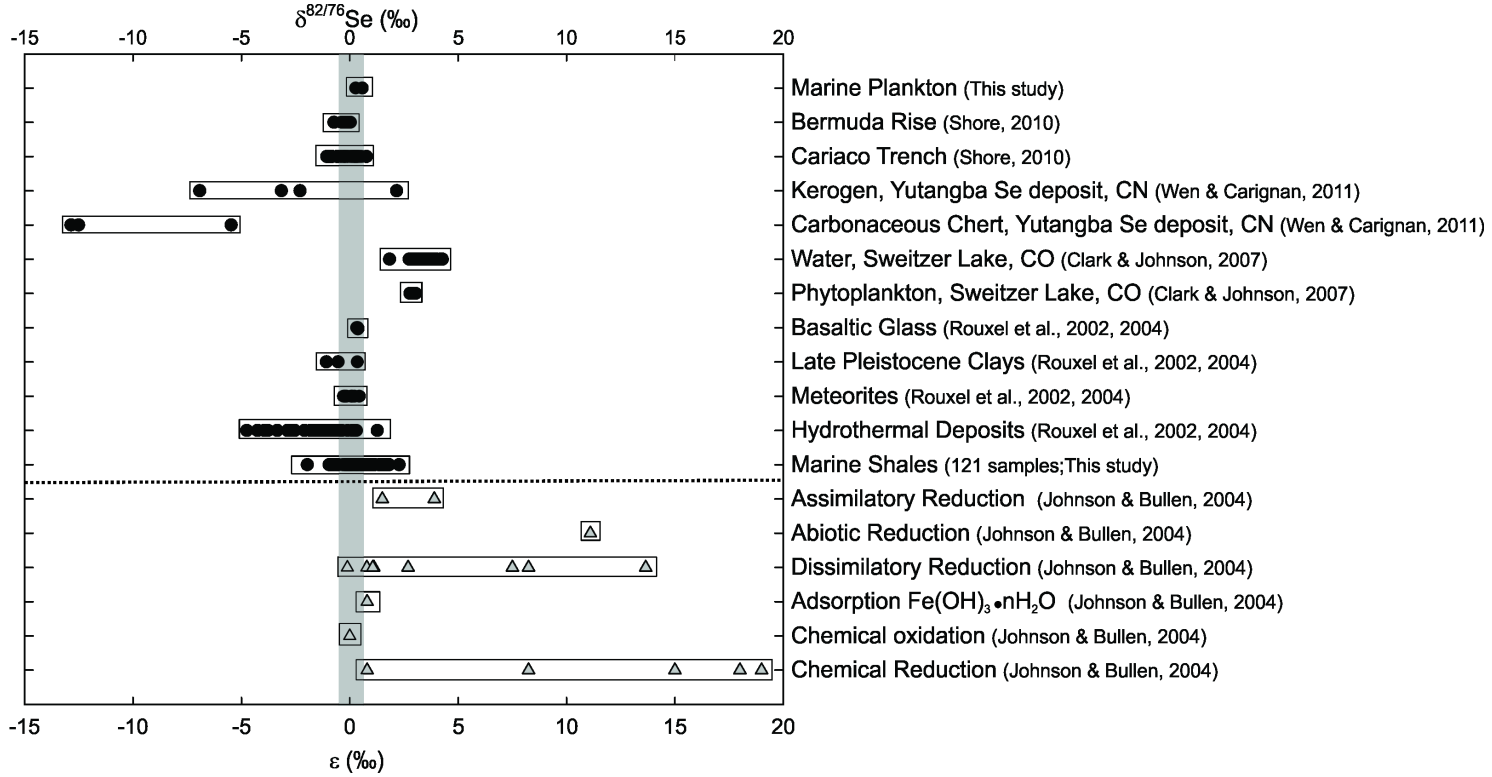

Figure 1 Compilation of $^{82/76}$Se isotope fractionation factors (ε; grey triangles) reported as $^{80/76}$Se by Johnson and Bullen (2004) and converted to $^{82/76}$Se using the relationship $\varepsilon_{80/76}=2/3\ \varepsilon_{82/76}$, and $^{82/76}$Se isotopic compositions (δ; solid circles) of natural materials. The latter include rocks, sediments, ore deposits, plankton and natural waters.

Isotope fractionation associated with assimilatory processes is often disregarded in traditional stable isotope studies, because they are generally small in comparison to isotope fractionation resulting from dissimilatory processes. The small fractionation during assimilatory sulfate reduction (1-5‰), for example, is attributed to the lack of exchange between internal and external sulfur pools (Canfield, 2001; Rees, 1973). However, as can be seen in Figure 1, in the selenium isotope system even small $\delta^{82/76}$Se fractionation during assimilatory reduction may be significant, because of the fairly narrow overall range of isotope fractionation, up to 15‰ for selenium compared to 72‰ for sulfur (Krouse and Thode, 1962; Tudge and Thode, 1950). There are only few studies of assimilatory Se reduction have produced isotope fractionation. One study found that algal uptake of selenate or selenite by the freshwater species *Chlamydomonas reinhardtii* results in $\varepsilon^{82/76}$Se values between 1.65 and 3.90‰ (Clark, 2007; Hagiwara, 2000).

This study focuses on selenium in well-characterized fine-grained marine sedimentary rocks, i.e., marine shales and mudstones, and their modern counterparts deposited from bottom waters exhibiting a range of redox conditions. The data are used to assess to what extent selenium concentrations and $^{82/76}$Se stable isotope ratios can be used as paleo-redox proxies.

CHAPTER 2. REVIEW OF SELENIUM BIOGEOCHEMISTRY

2.1 Selenium Cycling

Selenium is situated between sulfur and tellurium in Group VIA of the periodic table. Although it has physical and chemical properties that are intermediate between those of metals and non-metals, it is usually characterized as a non-metal. There are several different allotropes of elemental selenium and three are generally accepted (Lide, 2006). These allotropes can have either an amorphous or crystalline structure. Amorphous selenium is red in powder form or black in vitreous form. Two major crystalline forms of selenium are monoclinic selenium (α and β forms) which is dark red, and hexagonal (trigonal) selenium which is a metallic grey and also the most stable form of selenium (Lide, 2006).

Selenium is one of the rarest trace elements in the crust with an average abundance of 0.05 g g^{-1}

(Taylor, 1964), and it is also unevenly distributed at the Earth's surface (Oldfield, 2002). Selenium can accumulate at high concentrations in ore deposits (e.g. coal), in hydrothermal fluids, in the run-off from irrigated seleniferous soils (e.g. Kesterson reservoir San Joaquin Valley, CA, USA) and in wastewaters generated by anthropogenic activity (Plant et al., 2003). Present day seawater has a Se/S ratio of $6.3x10^{-8}$ g/g and Mid-Ocean Ridge Basalt (MORB) has a ratio of $1.5x10^{-4}$ g/g (Rouxel et al., 2004). Although there are instances where selenium and sulfur behave similarly, the variation in the Se/S ratios illustrates that the two element cycles are often decoupled.

Seawater selenium concentrations are very low (Scheinost and Charlet, 2008) and can be variable depending upon location. Selenium exhibits nutrient-like distribution in the water column, with very low concentration at the surface due to biological scavenging with regeneration at increased depth (e.g. Cutter and Cutter, 1995; Johnson, 2004; Measures et al., 1983). It has been reported that organic selenide may be taken up by marine phytoplankton as a recycling mechanism in the surface ocean (Baines, 2001). Organically bound selenium that settles out of the surface ocean is rapidly recycled at a rate of 1.6 pmol Se L-1 year-1 (Cutter and Bruland, 1984).

Biological processes are a major source of selenium emissions to the atmosphere. Both land plants and phytoplankton emit volatile selenium compounds including dimethyl selenide (DMSe) and dimethyl diselenide (DMDSe). DMSe is thought to be the main form of volatile selenium that reaches the atmosphere (Wen and Carignan, 2007). Production of methylated selenium compounds by the marine biosphere represents the main input of selenium to the atmosphere, with a flux from 5 to $35x10^{9}$g Se yr^{-1} (Amouroux and Donard; Amouroux et al., 2001; Mosher and Duce, 1987). Dimethyl selenide is highly reactive and the residence time for DMSe in the atmosphere is estimated to be 6 hours (Atkinson et al., 1990). The present day Se/S ratio of volatile components ($1.5x10^{-4}$) (Amouroux et al., 2001) is similar to historical values (800 B.C. to 1892) of Se/S found in Greenland ice cores ($1.4x10^{-4}$) (Weiss et al., 1971).

Selenium can be transported to marine sediments via several pathways. The major supply of selenium to marine sediments appears to be the deposition of organic detritus at the seafloor (Baines and Fisher, 2001; Cutter and Bruland, 1984; Ohlendorf, 1989; Wrench and Measures, 1982). The present-day

deposition flux of selenium is estimated to range from $7.4x10^9$ to $1x10^{10}$ g Se/year (Wrench and Measures, 1982). A study of riverine sediments suggests that the predominant species may be recalcitrant organic selenium or Se(IV) adsorbed to organic materials (Oram et al., 2008). These could be important inputs to marine sediments as well.

Adsorption of selenium anions is also thought to be an important source of selenium to marine sediments. Selenate and selenite anions are known to adsorb to organic matter, iron oxides and iron sulfides (Balistrieri and Chao, 1987; Bruggeman et al., 2005; Scheinost and Charlet, 2008). Selenite forms strong inner-sphere complexes with α-FeOOH (goethite), making it more immobile than selenate which forms weak outer-sphere complexes with goethite (Hayes et al., 1987). The adsorption of selenium oxyanions on goethite depends on several factors including other anions present, especially phosphate and organic acids (Balistrieri and Chao, 1987). The pH during deposition also plays a large role in mobility of selenite which is strongly adsorbed at low pH and becomes more mobile with increasing alkalinity up to pH 11 when it becomes completely dissolved (Howard III, 1977; Neal et al., 1987). Selenite, but not selenate, has been shown to adsorb to humic substances forming organically bound selenium, humic substances appear to disrupt the formation of elemental selenium (Bruggeman et al., 2007; Bruggeman et al., 2005). Adsorption of selenite on FeS_2 results in the subsequent reduction of selenite to elemental selenium (Bruggeman et al., 2005). Selenite also adsorbs to mackinawite (FeS) and is reduced to either elemental selenium or Se (-II) in the form of FeSe depending mainly on pH (Scheinost and Charlet, 2008). Adsorption of selenite to siderite appears to result in only minimal reduction to elemental selenium, with most of the selenite remaining adsorbed (Scheinost and Charlet, 2008). Magnetite to reduces selenite to Se(-II) after adsorption forming an unidentified mixed valence (Fe(II)-Fe(III)) iron selenide (Scheinost and Charlet, 2008).

2.2 Redox pathways

2.2.1 Major redox states

Selenium has several oxidations states, the main ones being –II, 0, IV and VI. In solution selenium generally occurs as selenate (SeO_4^{2-}), and selenite (SeO_3^{2-}). Selenate is more bioavailable than

selenite due to selenite's tendency to adsorb strongly to soil particles (Neal and Sposito, 1989; Neal et al., 1987). There are also several organic compounds that are highly bioavailable, including selenomethionine and selenocystine, these compounds are two to four times more bioavailable to plants than selenite (Mayland, 1994). Elemental selenium is non-toxic and immobile, making its biological significance negligible. Hydrogen selenide is toxic to humans at a concentration as low as 1.5 ppm (Lide, 2006). Redox species of selenium are often found in association with each other. For example, elemental selenium found in oxic waters with Se(IV) and Se(VI), though theoretically elemental selenium is not stable under these conditions (Tokunaga et al., 1991; Zawislanski, 1998; Zhang and Moore, 1996). Thus, selenium often defies equilibrium redox speciation in nature.

2.2.2 Assimilatory reduction

Selenium has been described as an 'essential toxin' that can be either a micronutrient or highly toxic to both prokaryotes and eukaryotes (Stolz et al., 2006). Selenium is an essential element due to its incorporation into selenocysteine (the 21st amino acid) a building block of selenoenzymes and is essential in over 20 selenoproteins (Böck et al., 1991). The gene coding for the synthesis of selenocysteine (SecS) has been found in eukaryotes (mainly mammals), eubacteria and archaea (Xu et al., 2007). Thioredoxin reductase is a major antioxidant enzyme into which selenocysteine is incorporated and is found in all branches of the tree of life (Gladyshev and Kryukov, 2001).

Uptake of selenate is thought to occur through the same channels as sulfate, as they have similar radii (covalent radii: S: 1.04 Å, Se: 1.17 Å) (Milne, 1998; and references therein). There is no direct evidence that selenite is taken into the cell intact; however, some organisms seem to have non-specific mechanisms to take up selenite while others have specific mechanisms (Milne, 1998; and references therein). Selenium can also be taken up in the form of dissolved organics, and this may be the dominant pathway of uptake in the surface oceans (Baines, 2001; Ohlendorf, 1989).

2.2.3 Dissimilatory reduction

Microorganisms capable of growth with selenium (IV, VI) as terminal electron acceptor can be placed in four groups, based on growth conditions and phylogeny: hyperthermophilic archaea,

thermophilic bacteria, mesophilic gram-negative bacteria, and γ-, δ- and ε-proteobacteria, shown in Figure 2 (J.S. Geelhoed, personal communication, 2007).

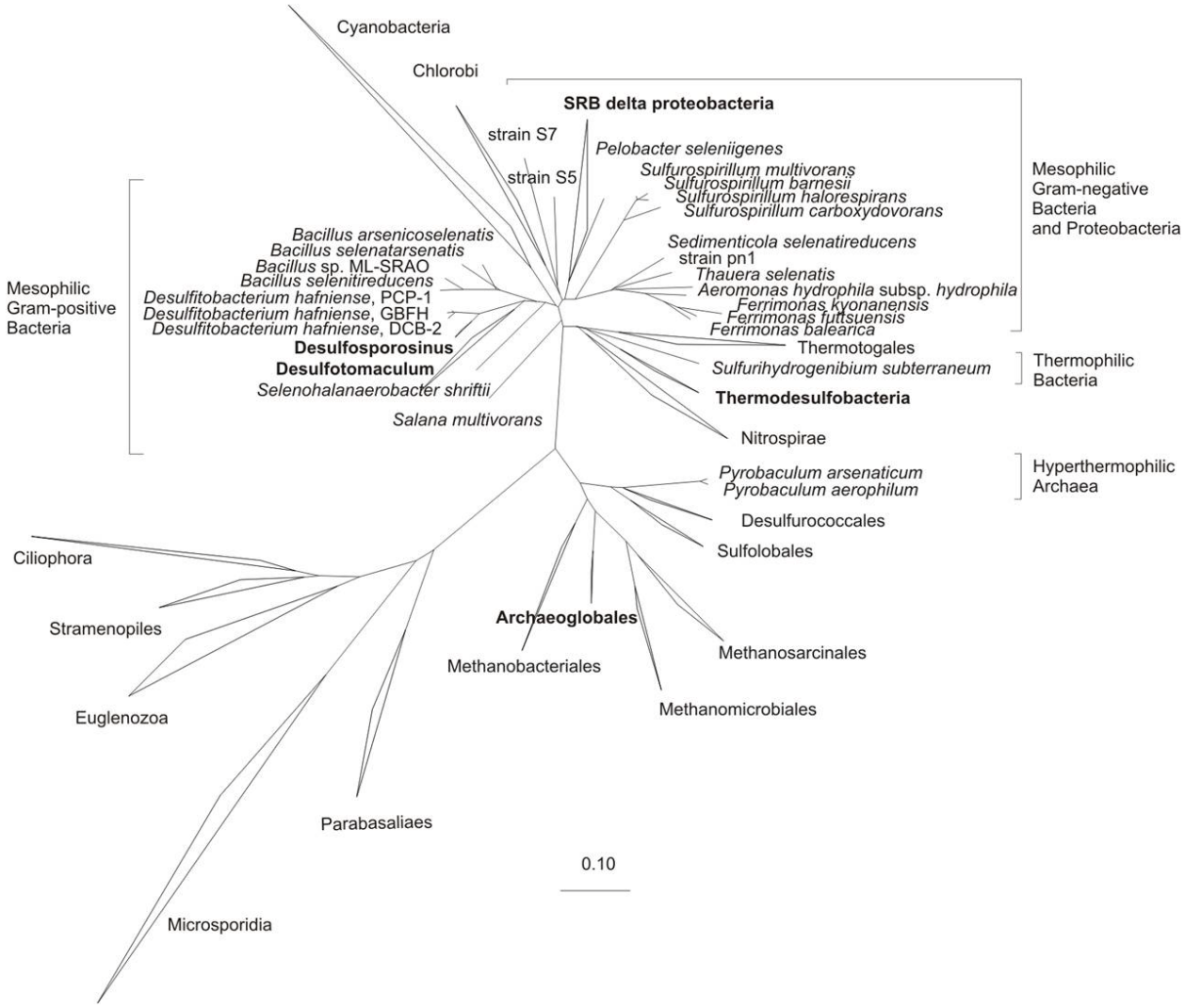

Figure 2 Phylogenetic tree showing all known Se reducing microorganisms that couple Se oxyanion reduction to growth (J.S. Geelhoed, personal communication). Species names are shown in italics.

The (hyper)thermophilic selenium reducers are able to use an autotrophic growth mechanism with H_2 or reduced sulfur compounds as electron donor, and *Bacillus sp.* ML-SRAO reduces Se(VI) with arsenite as electron donor. Of the mesophilic organisms, *Sulfurospirillum* species may use an inorganic electron donor in the form of hydrogen, but require an organic carbon source for growth. Thus far, the

selenate reductase enzyme has only been isolated from *Thauera selenatis* (Schroder et al., 1997).

Another mechanism by which selenium oxyanions are reduced is co-metabolic reduction. For this process, energy in the form of an electron donor is required, however, the selenium reduction process is not coupled to growth (e.g. Tomei et al., 1995). Several mechanisms have been proposed and these include the reduction of selenium oxyanions by the activity of reduction enzyme systems for other anions, such as nitrite and nitrate reductases, and the reduction of Se(IV) by glutathione (DeMoll-Decker and Macy, 1993; Kessi and Hanselmann, 2004). Reduction of selenium oxyanions by a non-specific reduction pathway has also been shown for some species of sulfate reducing bacteria affiliated with the δ-proteobacteria (Hockin and Gadd, 2006; Zehr and Oremland, 1987). Experiments with strains of *Desulfovibrio desulfuricans* and *Desulfomicrobium* suggest that selenate disrupts sulfate uptake mechanism and thus are likely reduced via the same pathway (Newport and Nedwell, 1988).

The predominant end product of the reduction of selenium oxyanions is red amorphous elemental selenium. However, formation of considerable amounts of Se(-II) has been observed for selenite reduction by *Bacillus selenitireducens*, *Citrobacter freundii* and *Veillonella atypica* (formerly known as *Micrococcus lactilyticus*) (Herbel et al., 2003; Pearce et al., 2008; Woolfolk and Whiteley, 1962; Zhang et al., 2004). The latter two organisms are able to reduce selenium oxyanions, but are unable to conserve energy for growth from this conversion. Production of Se(-II) occurs only after all selenite has been converted to Se(0).

Elemental selenium is mainly deposited outside the cell. Therefore, it is likely that reduction of Se(0) to Se(-II) is achieved via a mechanism of extracellular electron transfer. This may involve electron shuttle compounds or extracellular proteins. The use of conductive pili structures for electron transfer has been proposed as well (see reviews by: Gralnick and Newman, 2007; Lovley and Phillips, 1994; Stams, 2006). Electron shuttle compounds are present in the natural environment, e.g. in the form of humic substances, reduced sulfur compounds, Fe-colloids, and compounds produced by microorganisms, e.g. phenazines and flavins.

Geobacter sulfurreducens is well known to use extracellular proteins (c-type cytochromes and

multicopper proteins) to transfer electrons to Fe-oxides and electrodes (Lovley, 2006). Although *G. sulfurreducens* does not respire selenium oxyanions, it can reduce Se(IV) to Se(-II) (Pearce et al., 2008). In addition, the presence of the electron shuttle compound and humic acid analogue anthraquinone disulfonic acid (AQDS) has been shown to speed up the reduction of selenite by *V. atypica* (Pearce et al., 2008). *Shewanella putrefaciens* strain 200 is known to reduce selenite (Taratus, 2000), and adsorb and subsequently reduce selenate at pH<6 (Kenward et al., 2006). The mechanism of reduction of selenite and adsorption of selenate are currently unknown. *S. putrefaciens* is also known to use c-type cytochromes to transfer electrons to Fe-oxides (DiChristina et al., 2005). It is possible that selenite reduction in *S. putrefaciens* could be carried out enzymatically or more likely is a result of reduction by iron (II) produced by electron shuttling (Taratus, 2000; T.J. DiChristina, personal communication).

2.2.4 Volatilization

Detoxification of selenium compounds by some organisms such as humans, rats and bacteria is well known with the evolution of dimethyl selenide and trimethyl selenonium ion are common in excretory products (Stadtman, 1990; and references therein). There are five forms of volatile selenium; hydrogen selenide (H_2Se), methane selenol (CH_3SeH), dimethyl selenide (CH_3SeCH_3; DMSe), dimethyl selenenyl sulfide (CH_3SeSCH_3) and dimethyl diselenide ($CH_3SeSeCH_3$; DMDSe) (Chasteen, 1998). The first two forms are rapidly oxidized under present atmospheric conditions. The last two forms have a low vapor pressure at low temperatures therefore selenium is not thought to be volatized in these forms. This leaves dimethyl selenide as the key compound for selenium mobility in the environment (Chasteen, 1998).

Bacteria, phytoplankton, and fungi appear to be major sources of volatilized selenium (Challenger and North, 1934; Chau et al., 1976). Land plants are often divided into two categories of selenium accumulator plants and non-accumulator plants. Selenium accumulator plants being able to reach internal levels of selenium 100-10,000 times the levels found in non-accumulator plants. It has been postulated that the volatilization may not be a process conducted by the plants at all, but may be due to the degradation of the plant tissues by bacteria (Chasteen, 1998; Gamboa-Lewis, 1976); however this is still a

point of debate. Mechanisms for selenium volatilization may be similar to or the same as those that methylate sulfur (Ansede and Yoch, 1997; Challenger and North, 1934; Gamboa-Lewis, 1976; Reamer and Zoller, 1980).

2.2.5 Microbial Oxidation

There are only three known selenium oxidizers *Bacillus megaterium, Thiobacillus ASN-1*, and *Leptothrix MNB-1* (Dowdle and Oremland, 1998; Sarathchandra and Watkinson, 1981). Elemental selenium can be oxidized to selenite and selenate (Dowdle and Oremland, 1998; Sarathchandra and Watkinson, 1981). The aerobic (oxidative) cycle of selenium does not seem to compete with that of sulfur, but appears to be a co-metabolic process (Dowdle and Oremland, 1998). Microbial oxidation of Se(0) is very slow when compared to the reduction of selenate (Dowdle and Oremland, 1998).

2.2.6 Reduction by iron (II) bearing minerals

Selenate and selenite can be reduced by Fe(II,III) oxides (green rust) that are found in suboxic sediments and soils (Myneni et al., 1997). However, green rust minerals are rarely abundant in natural reductive environments due to their metastability with respect to magnetite and siderite (Charlet et al., 2007). A recent study of selenite reduction by mackinawite, siderite and magnetite found multiple reaction products including FeSe, Se(0) and mixed valence iron selenides (Table 1) (Scheinost and Charlet, 2008). Reduction of selenite by mackinawite produces different end products depending on the starting pH; at pH 4.4 FeSe forms, and at pH 6.3 elemental selenium forms. This suggests that the solubility of mackinawite at different pH values supplies the Fe(II) in solution for the precipitation of FeSe. The solubility of mackinawite is highly sensitive to pH, with the solubility increasing with decreasing pH (Rickard, 2006).

Table 1 Reaction products of selenite reduction with iron minerals

Iron Mineral	pH	Reaction product
Mackinawite (FeS)	4.4	FeSe
Mackinawite(FeS)	6.3	Se(0)
Siderite ($Fe^{II}CO_3$)	8	$Fe^{II}Fe^{III}_2Se_8$
Magnetite ($Fe^{II}Fe^{III}_3O_4$)	6	$Fe^{II}Fe^{III}_7Se_8$

Reaction rates of selenite with mackinawite and selenite with magnetite are fairly fast, occurring

within hours. The specific surface areas of the mineral phases appear to be one of the controlling factors of the reaction rates. Though reaction rates are very fast under experimental conditions it is likely that they are in competition with other processes such as adsorption on clay minerals or humic substances in natural settings and thus reaction rates may be slower (Bruggeman et al., 2005; Scheinost and Charlet, 2008).

2.2.7 Reduction by aqueous sulfide and iron sulfide

The precipitation of elemental selenium and sulfur has been observed in cultures of *Desulfomicrobium norvegicum*, which was isolated from an estuarine sediment (Hockin and Gadd, 2003). However, it was proposed that the reduction mechanism was abiotic reduction of selenite ions by aqueous sulfide (Equation (1)), rather than reduction by ferrous iron. It was further argued that the reduction of selenite is favored over the formation of iron mono-sulfide (Equation (2)).

$$SeO_3^{2-} + 2HS^- + 4H^+ \rightarrow Se^0 + 3H_2O \quad \Delta G^\circ = -324.3 \text{ kJ/mol} \tag{1}$$

$$Fe^{2+} + S^{2-} \rightarrow FeS \; \Delta G^\circ = -108.4 \text{ kJ/mol} \tag{2}$$

Reaction (1) has been independently verified by mixing Na_2SeO_3 and Na_2S in a carbonate buffered solution at pH 8.2 (Breynaert et al., 2008).

Iron sulfides also appear to reduce selenite in solution given a sufficient equilibration time of 2-3 weeks (Breynaert et al., 2008). The reduction of selenite by FeS appears to be the result of the dissolution of FeS and subsequent reaction between selenite and sulfide in solution which produces suspended colloidal Se(0) as an intermediate, with an end product attributed to $FeSe_x$ species (Breynaert et al., 2008). The reaction with FeS_2 appears to produce monoclinic elemental selenium, as opposed to trigonal elemental selenium (Breynaert et al., 2008). It is unclear what the exact mechanism for reduction is in the presence of pyrite, although surface precipitation has been ruled out as there is no iron in the final product (Breynaert et al., 2008). The reduction of selenite by pyrite has also been studied in the presence of humic substances and appears to increase the initial kinetics of the reaction due to increased mobility and availability of Fe(II), which also implies a different mechanism for reduction (Bruggeman et al., 2005).

2.2.8 UV transformations of Se

Photo-oxidation of Se(IV) oxyanions by UV radiation has been observed in the laboratory at a wavelength of 300 nm by Chen et al. (2005). The authors investigated the oxidation of Se(IV) in several different matrices, including pure water, HNO_3, HCl and a mixture of HCl and HNO_3. In pure water the rate of oxidation was relatively slow, with only 60% oxidation observed after 5 hours. In contrast, in 1% (v/v) HNO_3, oxidation was 100% complete within 60 minutes. The relative roles of pH and nitrate on the photochemical oxidation kinetics remain to be determined.

The photo-reduction of selenium oxyanions has been studied in more detail than its counterpart, photo-oxidation (Nguyen et al., 2005; Tan et al., 2003a, b, c). The existing studies demonstrate that selenate and selenite ions can be photo-chemically reduced to Se(0) at wavelengths below 380 nm, in the presence of formic acid and using TiO_2 as a catalyst (Kikuchi and Sakamoto, 2000), with the reaction proceeding through several steps.

2.3 Selenium stable isotope fractionation

2.3.1 Isotope fractionation theory

Standard isotope notation will be used throughout the proposal. The isotope notation used for the selenium system is identical to that used by Canfield (2001). The fractionation factor is defined as follows:

$$\alpha_{(A\text{-}B)} = \frac{\left(\frac{^{82}Se}{^{76}Se}\right)_A}{\left(\frac{^{82}Se}{^{76}Se}\right)_B} \quad (3)$$

where A is the reactant and B is the product. Isotopic compositions are expressed as per mil (‰) and are presented in the standard delta notation reporting the 82/76 ratio relative to the NIST SRM 3149 standard:

$$\delta^{82/76}Se_{NIST} = \left[\frac{\left(\frac{^{82}Se}{^{76}Se}\right)_{Sam}}{\left(\frac{^{82}Se}{^{76}Se}\right)_{Std}} - 1\right] * 1000 \quad (4)$$

Fractionations are expressed in terms of ε, also with units of (‰):

$$\varepsilon_{A\text{-}B} = 1000*(\alpha_{A\text{-}B} - 1) \quad (5)$$

The epsilon notation is convenient because ε is roughly equal to the difference between the δ values for two compounds:

$$\varepsilon_{A\text{-}B} \cong \delta^{82/76}Se_A - \delta^{82/76}Se_B \quad (6)$$

The ε reported here correspond to the 82/76 ratios relative to the NIST SRM 3149 standard ($\varepsilon^{82/76}Se$).

The majority of the redox reactions that impart relatively large isotope fractionations are kinetic, multi-step reactions that occur at low temperatures. Such is the case for selenium isotope fractionation. The mechanisms of selenium oxyanion reduction are not well understood, especially for dissimilatory reduction of selenate and selenite (see section 2.2.3). However, much of selenium isotope theory is based on that of sulfur isotopes, specifically following the Rees (1973) model, which has been further expanded upon by others (Canfield, 2001; Canfield et al., 2006; Hoek et al., 2006; Mitchell et al., 2009). Only a simplified model is considered here; see the aforementioned references for further discussion.

$$SO_{4\,(out)}^{=} \xrightarrow{1} \left[SO_{4\,(in)}^{=} \xrightarrow{ATP\downarrow\ 2} APS \xrightarrow{e-\downarrow\ 3} SO_3^{=} \right] \xrightarrow{e-\downarrow\ 4} H_2S \quad (7)$$

In this reaction network the cell actively takes up sulfate via membrane-bound transport proteins (Equation (7); step 1), and this step is thought to be reversible (Cypionka, 1991) allowing exchange of sulfate in and out of the cell. A small isotope effect of -3‰ ($\varepsilon SO_{4(out)}$- $SO_{4(in)}$) is associated with this step (Rees, 1973). Once sulfate enters the cell it is activated by ATP via ATP sulfurylase to form adenosine 5'-phosphosulfate (APS) (Equation (7); step 2), which is reduced to sulfite by adenylsulfate reductase (Equation (7); step 3). These two steps are also considered to be reversible. No fractionation is expected during the activation of sulfate, but a 25‰ isotopic fractionation ($\varepsilon SO_4 - SO_3$) is assigned to APS reduction (Harrison and Thode, 1957; Harrison and Thode, 1958). The final reduction of sulfite to hydrogen sulfide is performed by sulfite reductase (Equation (7); step 4). A 25‰ isotope fractionation ($\varepsilon SO_3 - H_2S$) has been ascribed to this step (Kemp and Thode, 1968; Rees, 1973). This model allows a

maximum fractionation of (-3+25+25=) 47‰. It is presumed that the dissimilatory reduction of selenate (and selenite) anions follows a similar multi-step enzymatic pathway and the model has therefore been applied to the selenium isotope system (Johnson and Bullen, 2004).

Krouse and Thode (1962) calculated equilibrium isotope fractionations for selenium isotopes undergoing various redox transformations. At 25°C, equilibrium fractionation ($\varepsilon^{82/76}$Se) for the transformation between selenate and selenide was calculated to be 33‰. This is significantly smaller than equilibrium fractionation of 75‰ for the reaction of sulfate to sulfide (Tudge and Thode, 1950). This suggests that the kinetic isotope fractionation observed for selenium should be smaller than that of sulfur because it is much heavier than sulfur (Schauble, 2004). Thus far observed selenium isotope fractionations support this theory.

The present and past selenium isotopic composition of seawater is currently unknown, which complicates the interpretation of selenium isotope fractionation observed in marine sedimentary rocks. Sample size and oxidation state considerations hamper efforts to constrain the selenium isotopic value of modern sea water. Selenium does not readily form selenate minerals, thus it is also difficult to constrain the geological isotopic signature of selenium, as its concentration in barites etc. is extremely low (<20 ppb Se) (Rouxel et al., 2004).

2.3.2 Biotic fractionation

2.3.2.1 Fractionation associated with assimilatory reduction

Assimilatory processes often impart only small fractionation in many isotope systems, such as sulfur. This is thought to be because of the lack of exchange between internal and external pools of an element (Canfield, 2001; Rees, 1973), thus no large fractionation (1-5‰) is observed.

Few studies of assimilatory reduction have produced isotope fractionation data to date. Algal uptake of selenium in the freshwater species *Chlamydomonas reinhardtii*, produces fractionations of $\varepsilon^{82/76}$Se=1.5 to 3.9‰ (Clark, 2007; Hagiwara, 2000). Selenium extracted from wetland plant tissues exhibit an isotopic fractionation ($\varepsilon^{82/76}$Se) of <1.5‰. Volatilization of selenium appears to show an even

smaller amount of fractionation, with soil microbes showing a maximum of ($\varepsilon^{82/76}$Se) 0.9‰, and samples of cyanobacteria, a maximum of ($\varepsilon^{82/76}$Se) 1.7‰ (Herbel et al., 2002; Johnson and Bullen, 2004; Johnson et al., 1999).

2.3.2.2 Fractionation associated with dissimilatory bacterial reduction

Selenium isotopic fractionations associated with dissimilatory reduction by microorganisms are larger than for assimilatory reduction. Most studies of isotope fractionation by dissimilatory selenate and selenite reduction have been done on pure cultures, showing large selenium isotope fractionation. Herbel et al. (2000) performed selenate and selenite experiments using growing cultures of *Sulfurosprillum barnesii* strain SES-3, *Bacillus selenitireducens* strain MLS10 and *Bacillus arenicoselenatis* strain EH1. In these experiments, low fractionations were observed at the beginning of the experiments ($\varepsilon^{82/76}$Se) 0.3-1‰, with fractionation increasing as the reaction proceeded. The final fractionation observed was 7.5‰ ($\varepsilon^{82/76}$Se) in the selenate experiments and up to ($\varepsilon^{82/76}$Se) 13.65‰ in the selenite experiments.

Table 2 Selenium isotope fractionations associated with biotic reduction of selenium oxyanions

Reduction	Organism	Fractionation ($\varepsilon^{82/76}$Se, ‰)	References
Assimilatory	algae; *Chlamydomonas reinhardtii*	1.5-3.9	Clark, 2007; Hagiwara et al., 2000
Assimilatory	higher plants	<1.5	Clark, 2007
Volatilization	soil microbes	max 0.9	Herbel et al., 2002; Johnson & Bullen, 2004
Volatilization	cyanobacteria	max 1.7	Johnson, 1999
Dissimilatory Se(IV) → Se(0)	*S. barnesii* strain SES-3, *B. arsenicoselenatis* strain EH1 and *B. selenitireducens*	max 13.65	Herbel et al., 2000
Dissimilatory Se(VI) →Se(IV)	*S. barnesii* strain SES-3, *B. arsenicoselenatis* strain EH1 and *B.selenitireducens*	max 7.5	Herbel et al., 2000
Dissimilatory	sediment slurry (mixed)	8.25	Ellis et al., 2003
Dissimilatory	sediment slurry (mixed)	1.11 to 2.69	Clark & Johnson, 2008
Dissimilatory	sediment slurry (un-mixed)	0.79	Clark & Johnson, 2008
Dissimilatory	Intact sediment core	-0.11 to 1.06	Clark & Johnson, 2008

Sediment slurry experiments of selenite reduction show fractionations that are similar to those measured in the pure culture studies ($\varepsilon^{82/76}$Se; 8.25‰) (Ellis et al., 2003). The selenium concentrations used in the slurry experiments were much lower, the lowest being 230 nmol/L but they are still well above the seawater concentration of selenium (~1 nmol/L). There also appeared to be no dependence of

fractionation on the concentration of selenium. This is a significant finding, as the selenium isotope theory is based heavily on that for sulfur isotope fractionation, and a dependence on the sulfate concentration for sulfur isotope fractionation has been observed (Habicht et al., 2002).

A recent study on an intact sediment core and mixed and unmixed sediment slurries found much smaller fractionation than previous slurry experiments and microbial cultures (Clark and Johnson, 2008). The mixed slurries exhibited fractionation ($\varepsilon^{82/76}$Se) from 1.11 to 2.69‰ in the aqueous selenate fraction (i.e. the selenate became heavier). The unmixed slurries produced even smaller fractionation ($\varepsilon^{82/76}$Se) 0.79‰. The intact sediment core underwent two loadings of selenium, and in the first loading the fractionation was quite small ($\varepsilon^{82/76}$Se) -0.11‰ and in the second loading the fractionation was closer to the mixed slurries ($\varepsilon^{82/76}$Se) 1.06‰. This study is important because it is the first that uses environmentally relevant samples and low selenium concentrations (960 nmol/L).

2.3.3 Abiotic fractionation

Although there have been several measurements of fractionation caused by abiotic reactions, most of these reactions were conducted under laboratory conditions that are not particularly environmentally relevant (i.e. with strong acids; Table 3) (Johnson et al., 1999; Krouse and Thode, 1962; Rashid and Krouse, 1985; Rees and Thode, 1966).

Table 3 Abiotic selenium isotope transformations and associated isotope fractionations

Se transformation	Method	Fractionation ($\varepsilon^{82/76}$Se, ‰)	References
Se(VI)→Se(IV)	8 M HCl @ 25°C	18	Rees & Thode, 1966
Se(VI)→Se(IV)	4N HCl @ 70°C	8.25	Johnson, 1999
Se(VI)→Se(IV)/Se(0)	Green Rust	11.1	Johnson, 2003
Se(IV)→Se(0)	Ascorbic acid or NH_2OH	15-19	Rees & Thode, 1966; Krouse & Thode, 1962; Rashid & Krouse, 1985; Webster, 1972
Se(IV) adsorption	$Fe(OH)_3$ in H_2O	0.8	Johnson, 1999
Se(IV)→Se(VI)	1M NaOH, 30% H_2O_2 24°C	~0	Johnson, 2004

Johnson and Bullen (2003) have conducted the only reductive abiotic fractionation study on an environmentally relevant reaction to date. They investigated the reduction of selenite by green rust (GR), an Fe(II)-and Fe(III) bearing mineral with sulfate layers, see discussion of this reaction above. A fractionation of $\varepsilon^{82/76}$Se=11.1‰, was observed in these reduction experiments, and was highly

reproducible in repeated experiments. Johnson and Bullen (2003) did not observe a relationship between reaction rate and isotope fractionation. Adsorption of selenite to amorphous iron oxyhydroxide causes a very small isotope fractionation Table 3. The chemical oxidation of selenite to selenate has been shown to have no isotope fractionation associated with it Table 3.

2.3.4 Selenium isotope fractionation in hydrothermal systems

Isotopic compositions as low as -5.5‰ ($\delta^{82/76}$Se) have been observed in hydrothermal systems (Rouxel et al., 2004; Rouxel et al., 2002). For all ranges of Se/S values, sulfides show enrichment in light selenium isotopes relative to basalts (Rouxel et al., 2004). There is no apparent relationship between selenium concentration and selenium isotope fractionation. However, it is inconclusive where the selenium isotope fractionation stems from. The Se/S ratios seem to be too small for hydrothermal fluids only, thus a second source of selenium depleted water is need to explain the concentration data. It is possible that fractionations could be occurring due to abiotic redox processes when seawater mixes with hydrothermal fluid or biotic fractionation could be carried out by microbes at low temperatures (Rouxel et al., 2004).

2.3.5 Observed fractionations in shales and marine sediments

The largest range of selenium isotope composition (δ) are found in the Yutangba Selenium Deposit, Hubei Province, China, with $\delta^{82/76}$Se ranges between -14.20‰ and 9.13‰ (Wen et al., 2007; Zhu et al., 2008). A model, as follows, has been proposed to account for the large selenium isotopic fractionation found in these samples. Selenium is mobilized via oxidation in the soil zone and along fast-flowing fractures to an unknown depth below the soil (~1 m). As the selenium seeps downward, eventually the water becomes anoxic, and precipitates Se(-II) producing a selenium enriched layer. Over time the oxic front migrates downward as the land surface is eroded and selenium is mobilized near the top and re-deposited deeper, and the total amount of accumulated selenium increases. It is likely the selenium in the high selenium layer has been remobilized several times which may increase the isotopic contrast and explain the unusually high selenium isotope fractionations observed in these samples. Drill core samples show the isotopic variation decreasing and minimizing to ~0‰ at about 50 m depth (Wen

and Carignan, 2007, 2011; Zhu et al., 2008).

Table 4 Selenium isotopic compositions of geological samples

Sample Type	Fractionation ($\delta^{82/76}$Se, ‰)	References
Hydrothermal	-5.5	Rouxel et al., 2002, 2004
Carbonaceous shale	-14.20 to 9.13	Wen and Carignan, 2007, 2011; Zhu et al., 2008
Carbonaceous chert	-12.86 to 4.93	Wen and Carignan, 2011
Kerogen	-6.92 to 7.52	Wen and Carignan, 2011
Marine sediments	-1.08 to 3.40	Rouxel et al., 2002
Marine sediments	-1.43 to 0.00	Hagiwara, 2000
Altered shale	-7.20 to 0.66	Hagiwara, 2000
Shale (outcrop)	-1.58 to 4.56	Hagiwara, 2000
Shale (core)	-1.67 to 0.53	Hagiwara, 2000
Chalk (core)	1.46	Hagiwara, 2000

Rouxel et al. (2002) found isotopic variation in marine sediments ranging from -1.08 to 3.40‰ ($\delta^{82/76}$Se). Hagiwara (2000) investigated altered and unaltered shale, and marine sediments and found variations ranging between -7.2 and 4.56‰ ($\delta^{82/76}$Se). These data sets are probably more representative of the fractionation that is imparted by fewer consecutive redox transformations that is seen in the Chinese shale samples.

CHAPTER 3. MATERIALS AND METHODS

3.1 Marine shales, mudstones, and ocean anoxic events

Shales are fine-grained sedimentary rocks commonly found throughout the geological record. A shale's color is often interpreted as an indicator of the oxygen level of the depositional environment. Black shales, for instance, have 'the sedimentological, paleoecological and geochemical characteristics associated with deposition under oxygen-deficient or oxygen-free bottom waters' (Tyson, 1987; Wignall, 1994; Table 1). The usually high organic carbon concentrations and increased burial rates of organic carbon associated with black shales have been proposed to result from 1) increased primary productivity, or 2) enhanced preservation of organic carbon due to anaerobic conditions (Arthur et al., 1987). Generally, some combination of these two factors are thought to accompany the formation of black shale sequences, though this is still a matter of debate (Jenkyns, 2010). Increased productivity may be caused by an increase in the availability of limiting nutrients due to increased supply from the continents or more efficient nutrient recycling in the oceans (Van Cappellen and Ingall, 1994, 1996; Wignall, 1994).

Enhanced respiratory oxygen demand resulting from the increased supply of organic matter may in turn explain the expansion of anoxic bottom waters (Wignall, 1994).

Table 5 Bottom water of oxygen levels and corresponding facies. After Tyson and Pearson (1991).

Oxygen (ml L^{-1})	Environment facies	Biofacies
8.0-2.0	Oxic	Aerobic
2.0-0.2	Dysoxic	Dysaerobic
2.0-1.0	Moderate	
1.0-0.5	Severe	
0.2-0.0	Extreme	
0.2-0.0	Suboxic	Quasi-anaerobic
0.0	Anoxic	Anaerobic

Periods of time when oxygen-depleted waters covered large areas of the seafloor are known as Oceanic Anoxic Events or OAEs. They are typically recognized by extensive black shale stratigraphic horizons transcending local basins (Schlanger and Jenkyns, 1976). Major Phanerozoic OAEs occurred during the Toarcian (~183 Ma), the Early Aptian (OAE1a; ~120 Ma), and the Cenomanian-Turonian (OAE2; ~93 Ma) (Jenkyns, 2010). Here, sedimentary sequences that comprise the following three OAEs are investigated: OAE2, the Toarcian OAE and the Steptoean Positive Carbon Isotope Excursion or SPICE. Also included in this study are samples from the New Albany Shale that were deposited under oscillating bottom water redox conditions, as well as modern sediments from the Black Sea and Arabian Sea (Figure 2). A modern plankton sample was also analyzed for the selenium isotope composition and Se/TOC ratio.

3.2 Modern oligotrophic plankton

A plankton sample was collected from the open Pacific Ocean (138.9999°W, 32.0002°N). The sample was collected using a net with a mesh size of 200μm on board the R/V Kilo Moana in July 2008. The sample was freeze-dried, and processed following the same procedures as the sediment samples.

3.3 Black Sea: modern euxinic basin

The Black Sea is the largest existing euxinic basin, and serves as an analogue for ancient deposition and preservation of organic matter under euxinic conditions (Lyons and Kashgarian, 2005).

The Black Sea represents a quasi-steady state system with anoxic deep-water replacement times on the order of 2,000 years. Numerous geochemical proxies have been validated in the Black Sea including reactive plus total iron concentrations and the degree of pyritization (Canfield et al., 1996; Lyons and Kashgarian, 2005; Raiswell and Canfield, 1998), molecular biomarkers (Sinninghe Damsté et al., 1993), and molybdenum isotopes (Arnold et al., 2004).

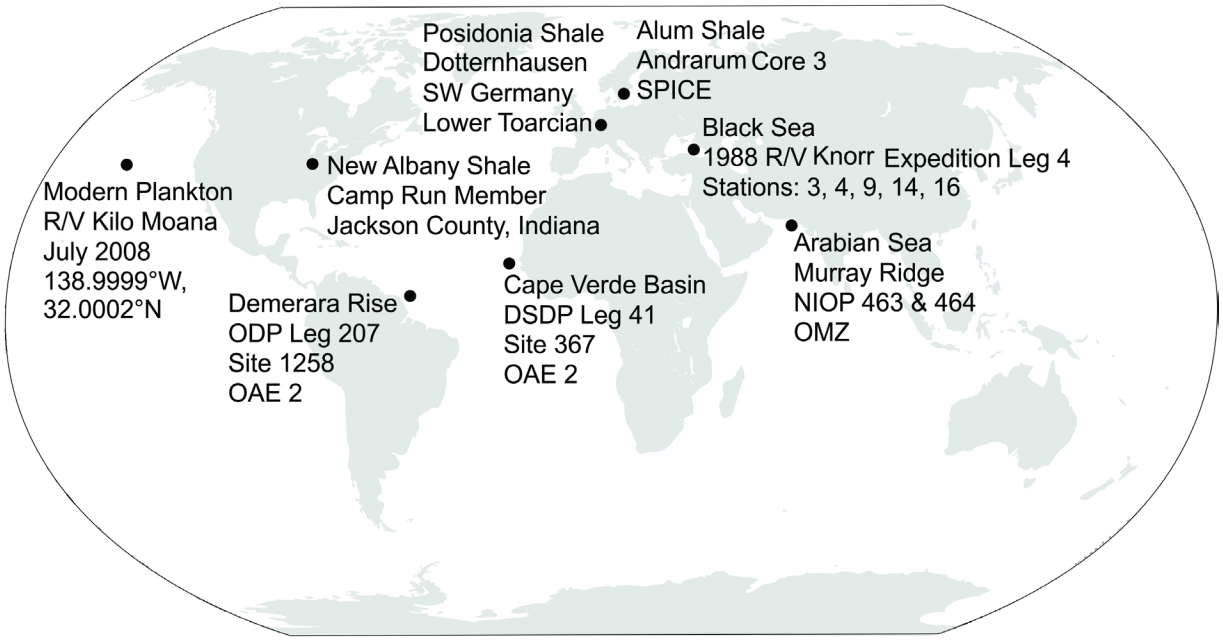

Figure 3 Sample locations and associated oceanic anoxic events. OMZ = oxygen minimum zone.

Black Sea sediments were collected on Leg 4 of the 1988 R/V Knorr Black Sea Oceanographic Expedition using a box core (Lyons, 1991; Lyons et al., 1993). Sediments deposited under oxic bottom waters have total organic carbon (TOC) contents of ~1 wt.%, those from the deep anoxic (euxinic) basin have significantly higher TOC contents of around 5 wt.%. The sediments are all of Holocene age. Sediment accumulation rates at the sites along the basin margin are on the order of 0.7 cm yr^{-1}, while at the sites in the deep (euxinic) basin the rates are around 0.02 cm yr^{-1} (Lyons and Kashgarian, 2005).

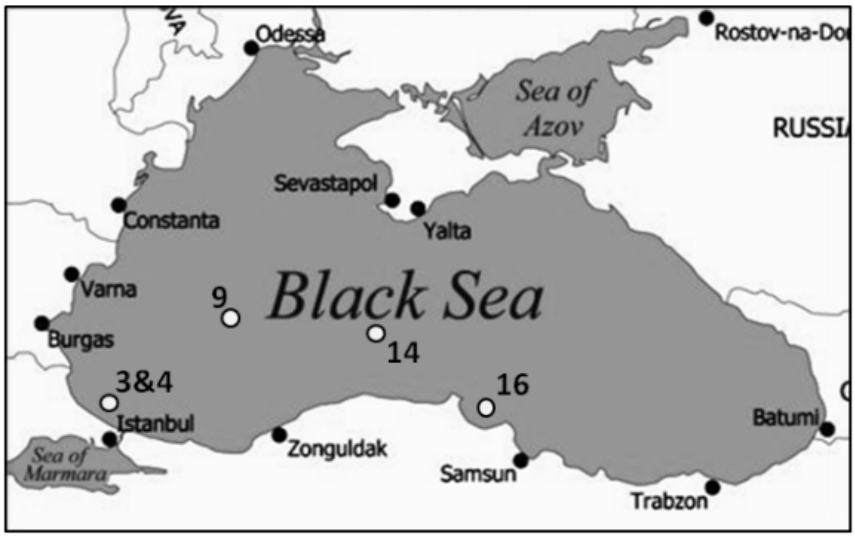

Figure 4 Black Sea: sites 9 and 14 are deep basin euxinic depositional environments, the other sites correspond to oxic settings on the shelf (sites 3 and 4) and in the Bay of Sinop (site 16). For further descriptions of the sites, see (Lyons, 1991).

3.4 Arabian Sea: modern oxygen minimum zone (OMZ)

Circulation in the Arabian Sea is controlled by seasonal shifts of the monsoon winds, causing upwelling of deep nutrient-rich water along both coasts of the Arabian Sea (Calvert et al., 1995). Increased productivity accompanies the seasonal upwelling of deep water. A strong oxygen minimum zone (OMZ) is present across the entire Arabian Sea at intermediate water depths (Calvert et al., 1995), with dissolved oxygen concentrations dropping to sub-oxic levels (~4.5 μM) (Morrison et al., 1999).

Sediment samples were taken from two piston cores (463 & 464) collected on Murray Ridge in the northern Arabian Sea during the Netherlands Indian Ocean Program (NIOP) in 1992. Core 463 is located within, core 464 below, the present-day OMZ. The geochemistry and chronology of the cores are described in detail elsewhere (Reichart et al., 1998; Sinninghe-Damsté et al., 2002; van der Weijden et al., 2006). The sediments used in the present study were deposited between 60 and 150 ky ago. The organic carbon profiles show precession-related variations that are more pronounced in core 463 than in core 464 (van der Weijden et al., 2006). The maximum TOC concentrations in core 463 are on the order of 6 wt.%.

3.5 Demerara Rise and Cape Verde Basin: OAE2

Sediment samples were obtained from ODP Leg 207 core 1258 on the Demerara Rise (Erbacher et al., 2005). The latter is a submarine plateau located in the western equatorial Atlantic Ocean, off the coast of Suriname. Cape Verde Basin sediments were collected during DSDP (Deep Sea Drilling Project) Leg 41 at Site 367 off the coast of Senegal (Kuypers et al., 2002). The sediments deposited during OAE2 are characterized by a distinct positive excursion of $\delta^{13}C_{org}$, with maximum values of -21‰. The entire $\delta^{13}C_{org}$ excursion is captured in the Demerara Rise core, but only the first half of OAE2 is recorded in the topmost portion of the Cape Verde Basin core.

The Demerara Rise sediments are mostly laminated black shales containing up to 29 wt.% TOC. The highest TOC concentrations coincide with the positive $\delta^{13}C_{org}$ excursion (Erbacher et al., 2005). The Cape Verde Basin sediments contain terrigenous silicates and clay minerals. High TOC concentrations of up to 40 wt.% are observed in the samples corresponding to OAE2 (Herbin et al., 1986; Kuypers et al., 2002). Further details on the trace element geochemistry of the sediments from both sites can be found elsewehere (Brumsack, 1986).

Organic matter in the Demerara Rise and Cape Verde Basin sediments is principally of marine origin (Erbacher et al., 2005). High rates of primary productivity (140-280 gC m^{-2} yr^{-1}) have been inferred for the Cape Verde Basin site prior to OAE2 (Kuypers et al., 2002). Organic matter accumulation rates at this site are estimated to have been on the order of 3 gC m^{-2} yr^{-1} before OAE2, that is, values comparable to those found in modern depositional environments underlying suboxic to anoxic bottom waters in areas of high productivity and high bulk sedimentation rates. During OAE2 the organic carbon accumulation rates increase to 9 gC m^{-2} yr^{-1}, or rates 3 times greater than prior to OAE2.

Anoxic water column conditions likely existed prior to OAE2, and often reached upward to the photic zone moving the chemocline significantly (Kuypers et al., 2002). Sulfidic conditions in the water column during OAE2 also appear to have reached the photic zone, and may have been present periodically before the anoxic event (Kuypers et al., 2002).

3.6 Posidonia Shale: (Early) Toarcian OAE

The Posidonia Shale was deposited in a shallow epicontinental sea and is characterized by very well preserved fossils and high TOC concentrations (Röhl et al., 2001). The samples for this study are from the Lower Toarcian black shale region in Dotternhausen, SW Germany, and span from the *Tenuicostatum paltum* layer to the *Bifrons commune* layer (Schmid-Röhl et al., 2002). The bottom 2 meters of the core consist of organic-poor (< 1 wt.% TOC) grey mudstones. The next 4.5 meters up-core comprise oil shales with very thin silty layers deposited during the Toarcian OAE; TOC concentrations are between 10 and 14 wt.% (GILL, 2010). The uppermost 1 meter of the oil shale shows evidence of bioturbation (Röhl et al., 2001). The topmost 2.5 meters of the core are mostly bituminous mudstones.

In contrast to OAE2, the Toarcian OAE is characterized by a negative shift in $\delta^{13}C_{org}$, with values as low as -34‰ (SCHMID-RÖHL et al., 2002). Two explanations have been proposed for the negative $\delta^{13}C_{org}$ shift. One relies on intense recycling within the organic-inorganic carbon system of a shallow stagnant basin (Schmid-Röhl et al., 2002), while the other one invokes the pulsed input of isotopically light carbon, presumably through volcanogenic CO_2 outgassing (Jenkyns, 2010).

The high degree of preservation of organic matter within the Posidonia Shale has generally been ascribed to the presence of permanently anoxic bottom waters. However, there are indications of short, intermittent periods of oxygenation during otherwise long periods of anoxia (Fisher and Hudson, 1987). A proposed mechanism for these oxygenation events are shifts between estuarine and anti-estuarine circulation (Röhl et al., 2001). During high river discharge accompanying monsoon rains, increased nutrient availability and decreased salinity led to the establishment of a redox boundary in the water column. This redox boundary persisted throughout the year when sea level stand was low. However, as sea level rose, the redox boundary was largely destroyed during the winter when anti-estuarine circulation dominated. Enrichment in trace metals supports a marked influence of fluvial input during Posidonia shale deposition (Brumsack, 1991).

3.7 New Albany Shale: stratified basin

Core material was obtained from the Camp Run Member of the New Albany Shale in Central Indiana (North American Exploration Hole INJK-I3 Sec. 9, T. 6N, R. 5E, Jackson County, Indiana). The core consists of alternating, and clearly separated, bioturbated and laminated shale layers. The laminated, black shales have relatively high TOC contents (average 8.2 wt.%) and their $\delta^{13}C_{org}$ values are on average 1.9‰ lighter than for the bioturbated layers (Calvert et al., 1996; Ingall et al., 1993). The bioturbated, grey shales show evidence of burrowing, and have low TOC contents (average 0.5 wt. %).

The Late Devonian-Early Mississippian New Albany Shale formed under conditions of eustatic sea level rise (Ingall et al., 1993). The geochemical characteristics of the Camp Run Member of the New Albany Shale indicate that the laminated shales were deposited under dysoxic to anoxic rather than euxinic conditions (Beier and Hayes, 1989). The repeated vertical shift of the anoxic/oxic interface at the basin margin is thought to have created the closely alternating layers of interbedded black and light colored shales (Calvert et al., 1996; Cluff, 1980).

3.8 Alum Shale: Upper Cambrian SPICE

The Scandinavian Alum Shale Formation, deposited during the Middle Cambrian to Lower Ordovician, consists mainly of dark grey to black mudstones and the Alum Shale. The latter is enriched in TOC (10–20%), syngenetic pyrite, phosphate and trace elements (Ahlberg et al., 2009). Together with the absence of bioturbation, this suggests anoxic conditions at the water-sediment interface during deposition of the Alum Shale. The fine-grained nature of the mudstones and shale suggests a depositional environment undisturbed by wave action, most likely a shallow, epicontinental shelf (< 200 m water depth) (Thickpenny, 1984). This depositional environment could have become severed from the open ocean causing stagnation within the basin and the development of anoxic bottom waters (Thickpenny, 1984). Bulk rock samples for this study were obtained from Andrarum-3 Drill Core in Sweden (Ahlberg et al., 2009).

The Late Cambrian SPICE (Steptoean Positive Carbon Isotope Excursion) has been observed in

several locations throughout the world, including Kazakhstan, China, Australia, Eastern and Western North America (Glumac and Walker, 1998; Saltzman et al., 1998). The widespread observation of this event it is thought to have been due to a global shift in carbon cycling, which also coincided with a global trilobite extinction event (Saltzman et al., 1998). Local euxinic conditions appear to have prevailed before and after SPICE, with a global spread of euxinic conditions during the event (Gill et al., 2011).

3.9 Plankton, sediment and rock digests

Freeze-dried plankton, rock or sediment powders were weighed to 0.5 g per aliquot. Each aliquot was pre-digested in a 7 ml PFA beaker with 2.5 ml of concentrated nitric acid at 100°C for 3 hours to oxidize the organic matter. After the pre-digestion the sample was transferred to a 23 ml PTFE liner using an additional 0.5 ml of concentrated nitric acid to rinse the PFA beaker (total of 3 ml HNO_3). The liner was then placed in a Parr bomb and heated to 165°C for 10 hours. After cooling down, the sample was moved to a 15 ml conical centrifuge tube and the PFA liner was rinsed with 1 ml H_2O; the rinse was also transferred to the centrifuge tube. The resulting suspension was centrifuged for 20 minutes at 3000 RPM, and the supernatant liquid was decanted into a clean 7 ml PFA beaker. The remaining rock or sediment powder was rinsed with 2 ml of 8 M HNO_3, and the powder was re-suspended by mixing on a vortexer. The suspension was centrifuged a second time using the same procedure, and the supernatant was added to the same 7 ml PFA beaker. The sample was then placed on a 100°C hot plate (inner beaker temperature ~70°C) and heated to incipient dryness. Once dry, the sample was re-suspended in 5 ml of 5 M HCl and ultra-sonicated for 15 min. Subsequently, it was filtered through a 0.45 μM pore size syringe filter and into a clean 30 ml borosilicate glass test tube with a PFA lined cap. The filter was rinsed into the same test tube using an additional 5 ml of 5 M HCl. The sample was then heated for 1 hour at 100°C in an aluminum block to convert any Se (VI) to Se (IV).

3.10 Analytical techniques

3.10.1 Selenium concentrations

After the digestion the total selenium concentration of each rock or sediment sample was determined via atomic fluorescence spectrometry (AFS). A small aliquot (900 µl) from the digest was diluted to a total of 20 ml with 30% HCl. The concentration was measured on a PSA 10.055 Millennium Excalibur Atomic Fluorescence Spectrometer equipped with a continuous flow hydride generator (HG) and a boosted discharge hollow cathode selenium lamp. The operational conditions are outlined in Table 2. The selenium concentration standard used was a single element ICP standard (1.000 µg mL^{-1} Se in dilute HNO_3, Ultra Scientific). The error associated with the method is ±2%.

Table 6 Operating parameters for total Se concentration measurements.

Sample flow rate (ml/min) (100%, Pump 1)	9
Reductant ($NaBH_4$) flow rate (ml/min) (100%, Pump 2)	4.5
Argon inner pressure (psi)	30
Carrier gas flow rate (Ar) (L/min)	0.3
Dryer gas flow rate (Ar) (L/min)	2.5
Measurement mode	Emission
Signal type	Peak height
Se Hollow cathode lamp primary current (mA)	20.0
Se Hollow cathode lamp boost current (mA)	25.1
Delay period (s)	15
Analysis period (s)	40
Memory period (s)	60

3.10.2 Selenium isotopic ratios

A thiol cotton fiber (TCF) was used for the chemical separation of selenium from the dissolved matrix (i.e., separation from Fe, Ge, etc.) for isotopic analysis. The preparation of the thiol cotton fiber followed a procedure modified after Yu et al. (2001). A mixture was prepared by combining 20 ml thioglycollic acid (96-99%), 14 ml acetic anhydride (99.9%), 6.4 ml glacial acetic acid, 0.064 ml sulfuric acid (97.5%) and 2.5 ml 18 MΩ water. Medical grade hydrophilic cotton (6 g) was added to the mixture. The separation of the selenium via the TCF used the detailed protocol described by Zhu et al. (2008).

Selenium isotope determinations were measured on a Hydride Generation Multi Collector Inductively Coupled Plasma Mass Spectrometer (HG-MC-ICP-MS), using a double focusing Nu Plasma

MC-ICP-MS (Wrexham, North Wales, UK), located at the Department of Geology, University of Illinois at Urbana-Champaign. The reductant used for the hydride generation was 0.3% $NaBH_4$ in 0.3% NaOH. The sample and reductant were introduced into the hydride generator at a flow rate of 0.25 ml min^{-1}. The hydrides generated were carried into the instrument with argon as the carrier gas.

The selenium isotope standard solution was NIST SRM 3149. The mass difference between ^{74}Se and ^{82}Se is ~10% but ^{74}Se is less abundant (0.87%) than ^{76}Se (9.02%), therefore even though the mass difference is smaller between ^{82}Se and ^{76}Se (~ 7%), the $^{82/76}Se$ ratio is preferable (Krouse and Thode, 1962). The low abundance of ^{74}Se also makes it ideal for the double spike technique used here. ^{74}Se-enriched and ^{77}Se-enriched spikes were purchased from ISOFLEX, USA, and mixed to create a selenium isotope double spike ($^{74}Se/^{77}Se$), which was added to all samples and well mixed prior to the TCF separation procedure. The samples for isotope analysis were prepared as to contain 4-6 μg ml^{-1} selenium, producing between 1.2 and 2 volts for ^{78}Se intensity. Between each sample the hydride generator apparatus was rinsed with 2 M HCl until the normal background signal was retrieved, in order to avoid memory effects between samples. An isotope standard was used approximately every 5 samples to account for instrument drift.

The analytical data were first corrected for interferences (for detailed discussion, see Zhu et al., 2008). The different isotopic ratios ($^{74}Se/^{78}Se$, $^{76}Se/^{78}Se$, $^{77}Se/^{78}Se$, $^{80}Se/^{78}Se$, and $^{82}Se/^{78}Se$) were then reduced using an iterative procedure to obtain the $^{82}Se/^{76}Se$ and $^{82}Se/^{78}Se$ ratios that were measured in the sample from the added double spike ratio. Selenium isotope ratios are reported relative to NIST SRM 3149.

CHAPTER 4. RESULTS

4.1 Average concentrations and isotopic compositions

We first provide a general overview of the dataset using average values of the total selenium concentrations and $^{82/76}Se$ δ values, together with average TOC concentrations and Se/TOC ratios (Figure 5). For each of the locations investigated, the samples are grouped in two or three categories described in

the following text. For the Black Sea, we separate the sediments from the oxic basin margin (white) from those collected in the deep euxinic basin (black). For the Arabian Sea, the two categories correspond to core 464 (white), excluding the bottom most sample that was deposited under anoxic conditions (Sinninghe-Damsté et al., 2002) and core 463 (black). For the Demerara Rise and Cape Verde Basin sediments, we distinguish the sediments that were deposited just before (white), during OAE2 (black) and after OAE2 (white). Similarly, for the Posidonia Shale and Alum Shale Formations, samples from before (white), during (black) and after (white) the Toarcian OAE and SPICE, are grouped together, respectively. Finally, for the New Albany Shale, the bioturbated and laminated shales define the two categories.

The average selenium concentrations vary by more than one order of magnitude (Figure 5A). Selenium concentrations in the Demerara Rise and Cape Verde Basin sediments are significantly higher than at the other sites. They are also well above the world shale average of 5 ppm (Turekian, 1961). As expected, for any given location, the sediments deposited under the more reducing conditions are on average more enriched in TOC (Figure 5B). The OAE2 sequences show the highest average TOC concentrations, and the lowest abundances are seen in the Black Sea plus Arabian Sea sediments and in the bioturbated layers of the New Albany Shale.

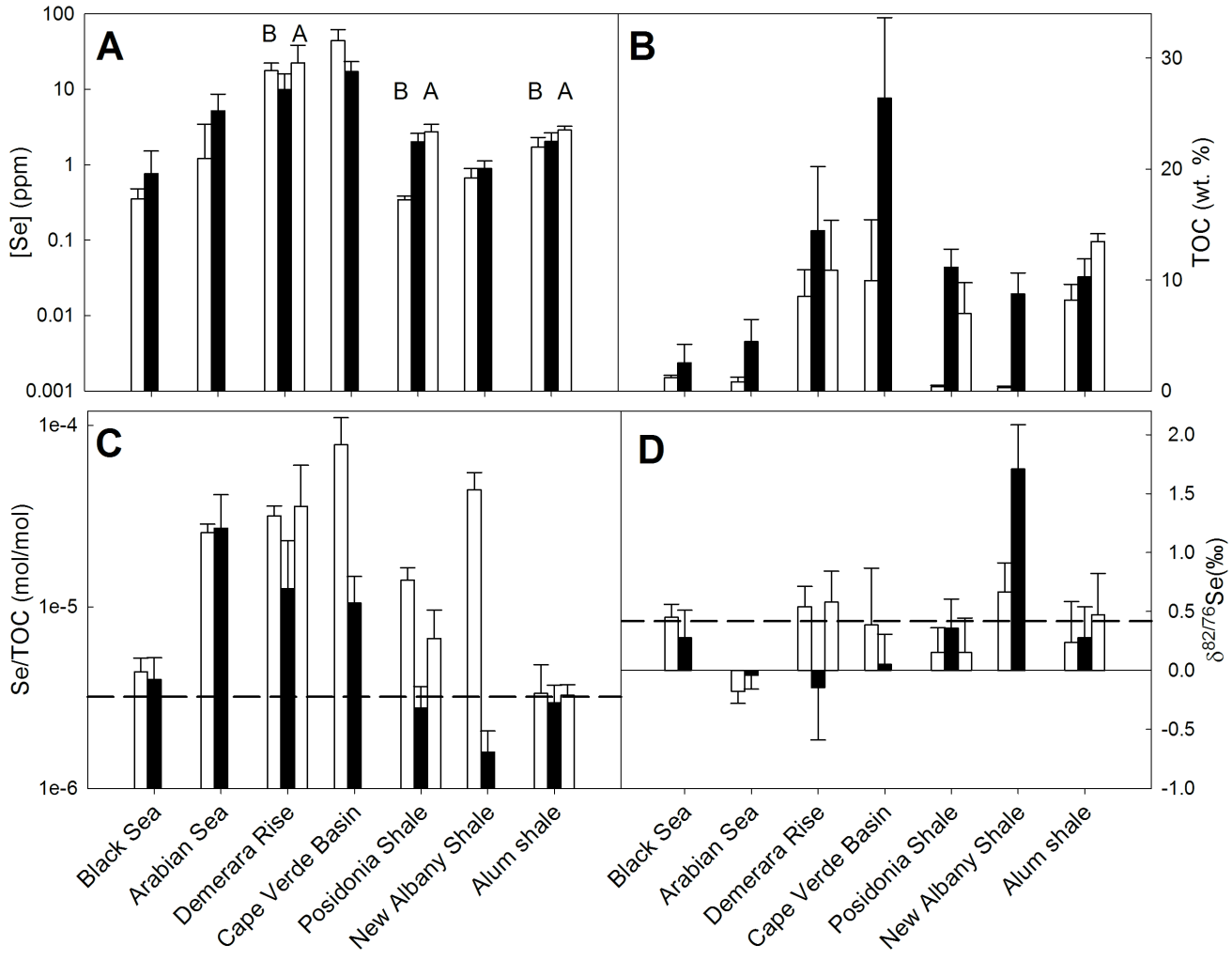

Figure 5 Average values of A) selenium concentrations (ppm) B and A stand for before and after OAE, respectively. And apply to all four graphs, B) total organic carbon, TOC (wt.%), C) Se/TOC ratios – the dashed line indicates the average Se:C ratio in phytoplankton (Doblin et al., 2006), and D) the $^{82/76}$Se isotopic composition (δ; ‰) – the dashed line indicates the isotopic composition of modern plankton from the open, oligotrophic Pacific Ocean. See text (section 4.1) for the definition of the sample categories for each of the locations. Error bars indicate standard deviations (1σ).

The selenium to organic carbon ratios (Se/TOC) vary by about two orders of magnitude (Figure 4C). The average Se/TOC values for the Black Sea sediments, the Alum Shale Formation, the Toarcian OAE and the laminated New Albany shale layers are close or slightly below the average value measured for modern marine phytoplankton ($3.2x10^{-6}$ mol/mol). The Arabian Sea cores, the non-OAE samples of the Demerara Rise and Cape Verde Basin and the bioturbated New Albany Shale layers have average Se/TOC ratios far above modern marine phytoplankton. Note, however, that the differences in average Se/TOC ratios between non-OAE2 and OAE2 sediments, and between the bioturbated and laminated layers of the New Albany Shale, are primarily due to concentration differences of TOC, rather than selenium (Figure 5A-C).

In contrast to the selenium concentrations and Se/TOC ratios, the average $\delta^{82/76}$Se values only exhibit a narrow range (-1.96 to 2.28‰, Figure 4D). Most values fall close to or below the isotopic composition of modern plankton (0.42‰) from the (open) Pacific Ocean (Figure 5D). The notable exceptions are the New Albany Shale with significantly heavier $\delta^{82/76}$Se values, and the Arabian Sea sediments and OAE2 samples from the Demerara Rise, which have negative average $\delta^{82/76}$Se values.

4.2 Black Sea

The selenium concentrations in the sediments from the oxic sites range from 0.22 to 0.49 ppm, with an average value of 0.35±0.13 ppm (1σ). For the deep basin sites, the corresponding range is 0.35 to 2.35 ppm, with an average concentration of 0.76±0.7 ppm. Although the average $^{82/76}$Se isotopic composition at the oxic sites is slightly heavier than at the deep basin sites (0.45±0.11‰ versus 0.29±0.28‰), the $\delta^{82/76}$Se ranges essentially overlap. Both the Se/TOC ratios and the $\delta^{82/76}$Se values of the Black Sea samples are comparable to the values measured on modern marine phytoplankton.

4.3 Arabian Sea

The data for both Arabian Sea cores are displayed in Figure 5. The selenium concentrations fall mostly in the range 1-4 ppm, except for sediments from the 100-125 kyr time interval in core 463, which

exhibit Se concentrations of up to ~11 ppm. Sediments from both cores show a very limited range in isotopic composition (< 0.5‰). The $\delta^{82/76}$Se values are among the most negative ones in the data set, with most values falling below 0‰. The molar Se/TOC ratios of the Arabian Sea sediments (2.01×10^{-5} to 3.44×10^{-5}) exceed that measured on marine phytoplankton (3.2×10^{-6}).

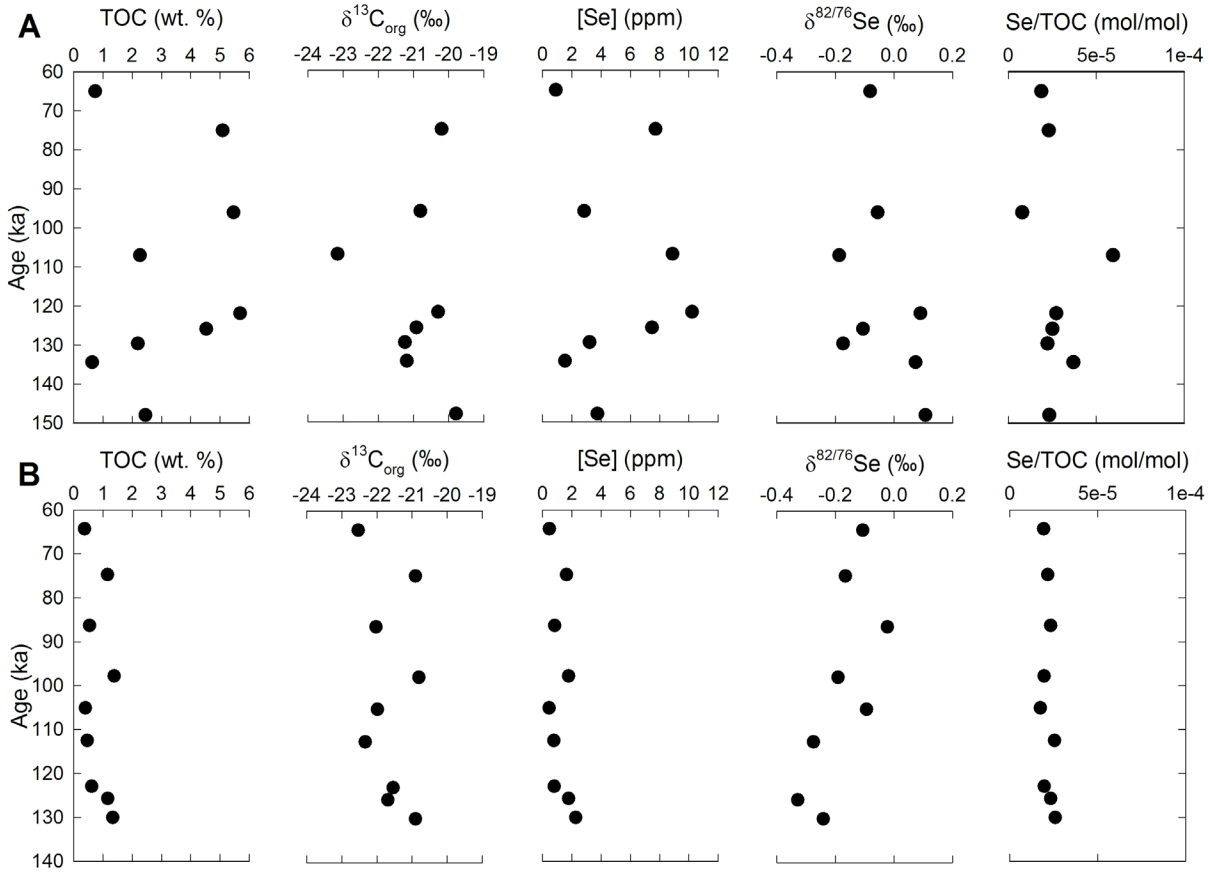

Figure 6 Arabian Sea data from A) NIOP Core 463 and B) NIOP Core 464 on the Murray ridge. For detailed descriptions of the sites, cores and δ^{13}C and TOC data, see (Reichart et al., 1997; Sinninghe-Damsté et al., 2002).

4.4 Demerara Rise and Cape Verde Basin

Very high selenium concentrations are observed in the Demerara Rise and the Cape Verde Basin samples (Figure 6), compared to the typical concentrations measured on the other rocks and sediment shales presented in this study. The maximum concentrations in the Demerara Rise (> 30 ppm) and Cape Verde Basin samples (> 70 ppm) are found after and before OAE2, respectively. During OEA2, the

selenium concentrations drop to values 2-3 times lower than those before and after the event. Together with the increase in TOC, this leads to a major drop in the Se/TOC ratios during OAE2.

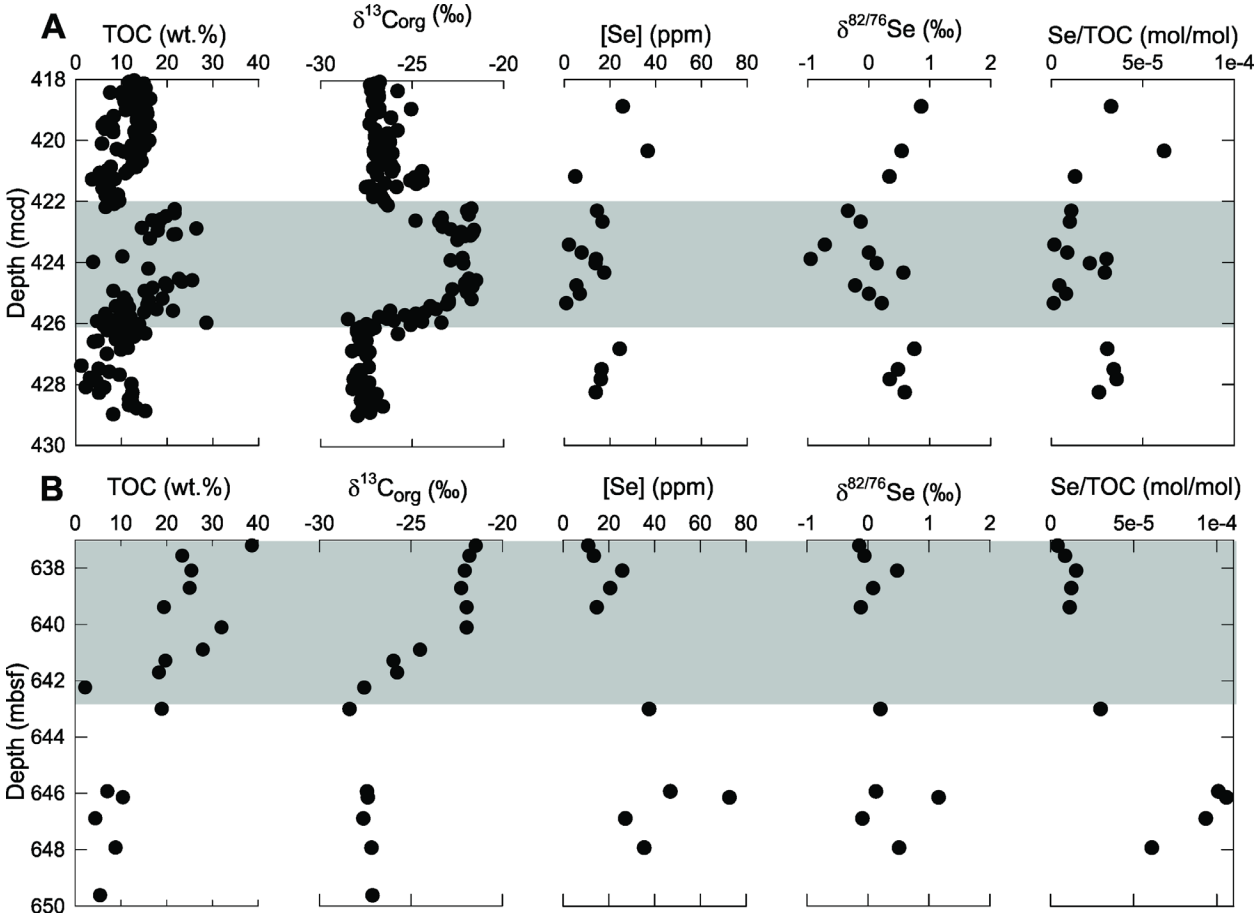

Figure 7 Data from the A) Demerara Rise and B) Cape Verde Basin cores. Grey bars indicate OAE2 as defined by the δ^{13}Corg excursion. Data for TOC and δ^{13}C for Demerara Rise are from Erbacher et al. (2005) and for Cape Verde Basin from Kuypers et al. (2002).

The shales deposited at Demerara Rise during OAE2 have the most negative $\delta^{82/76}$Se compositions of the entire dataset collected in this study, with a minimum $\delta^{82/76}$Se value of -0.72 ‰. The Demerara Rise core also shows the largest isotopic shift between samples. The average $\delta^{82/76}$Se during OAE2 is -0.14±0.45 ‰; before the event it is 0.54±0.17 ‰ and after the event 0.58±0.26 ‰. The general trend in $\delta^{82/76}$Se in the Cape Verde Basin core is similar, but less pronounced, than for the Demerara Rise. The average $\delta^{82/76}$Se values before and during OAE2 are 0.39±0.48 ‰ and 0.05±0.26 ‰, respectively.

Note, however, that only the lower portion of OAE2 is captured by the available Cape Verde Basin core material; that is, the data may not be representative for the entire OAE2.

4.5 Posidonia Shale

If we exclude the organic-poor mudstones at the bottom of the core, the selenium concentrations and isotopic compositions vary little along the core (Figure 8). The selenium concentrations tend to be slightly lower during the OAE (average: 2.01±0.59 ppm), compared to after the event (average: 2.72±0.70‰). The Se/TOC ratios are distinctly lower during the Toarcian OAE, primarily because of the higher TOC concentrations. The $\delta^{82/76}$Se values range over approximately 1‰ and are, on average, higher during (0.36±0.25‰) than before (0.15±0.21‰) or after the event (0.15±0.29‰).

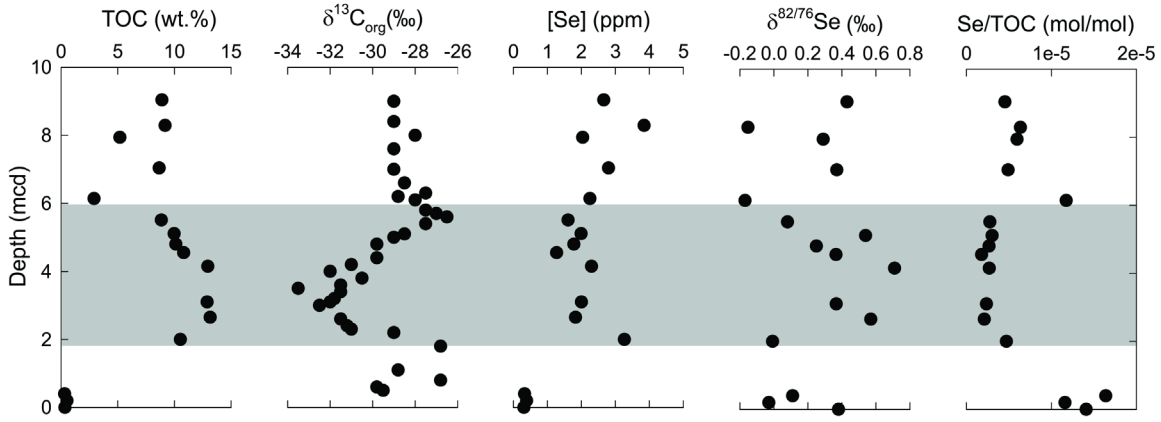

Figure 8 Posidonia Shale. Grey bar indicates Toarcian OAE based on $\delta^{13}C$ values, see text for description of negative $\delta^{13}C$. TOC data from B. Gill, personal communication and $\delta^{13}C_{org}$ data from Schmid-Röhl et al. (2002).

4.6 New Albany Shale

On average, the bioturbated grey shales have slightly lower selenium concentrations than the laminated black shales (0.67±0.28 versus 0.89±0.12 ppm) (Figure 9). The Se/TOC ratios are much higher in the bioturbated layers, however, because of the much lower TOC concentrations. Systematic differences in the selenium isotopic compositions are also observed between shale layers deposited under oxic and anoxic conditions: bioturbated shales are lighter with an average $\delta^{82/76}$Se value of 0.67±0.80‰

versus 1.71±0.48‰ for the laminated shales.

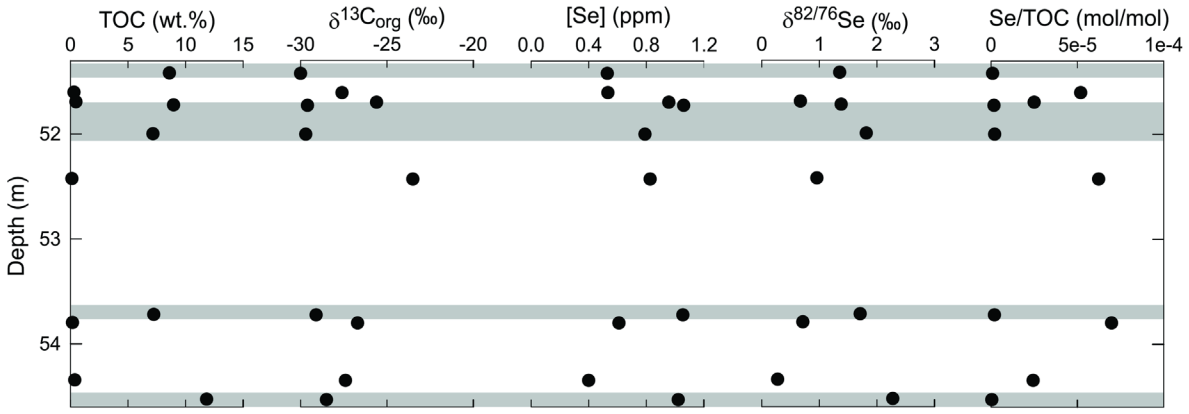

Figure 9 New Albany Shale. Grey bars indicate laminated black shales; white sections indicate bioturbated grey shales. $\delta^{13}C_{org}$ and TOC data are from Ingall et al. (1993) and (Calvert et al., 1996) respectively.

4.7 Alum Shale

SPICE is accompanied by a lowering of the selenium concentrations and $\delta^{82/76}$Se values (Figure 10). The average selenium concentration during the event is 2.03±0.61 ppm. Before SPICE the average concentration is 1.71±0.60 ppm, while after SPICE it increases to 2.88±0.35 ppm. The molar Se/TOC ratios remain fairly constant along the core ($3.33x10^{-6}$±$1.47x10^{-6}$ to $3.26x10^{-6}$±$4.77x10^{-7}$), with values close to those of modern marine phytoplankton. The selenium isotopic composition at the bottom of the core is relatively light ($\delta^{82/76}$Se = 0.24±0.35‰). The $\delta^{82/76}$Se values increase before the anoxic event, with a peak value at 0.79‰. Within SPICE, $\delta^{82/76}$Se values exhibit a local minimum that coincides with the maximum in $\delta^{13}C_{org}$ and the minimum in selenium concentration. The average $\delta^{82/76}$Se during SPICE is 0.28±0.26‰. After SPICE, $\delta^{82/76}$Se increases to 0.65±0.06‰.

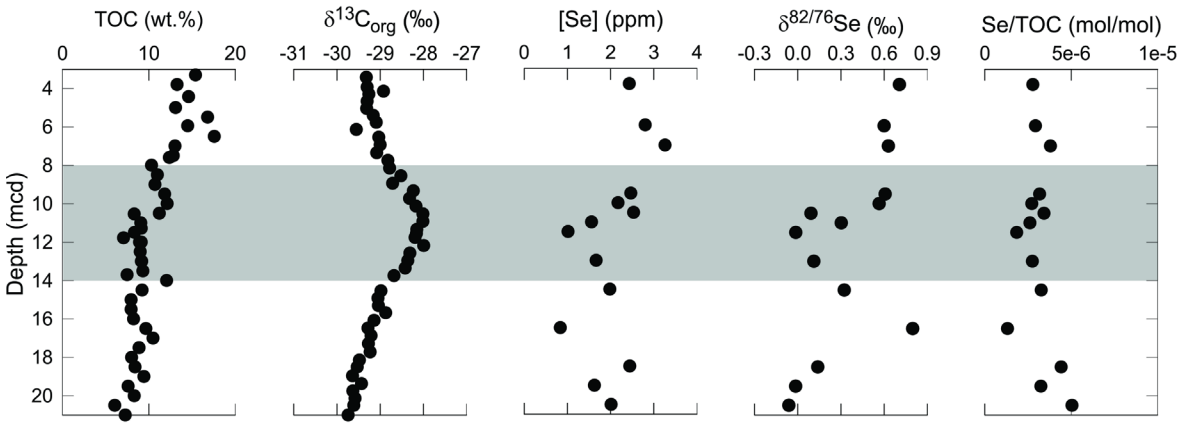

Figure 10 Alum Shale. Grey bar indicates the SPICE event based on $\delta^{13}C$ data. Data for TOC and $\delta^{13}C_{org}$ from Ahlberg et al. (2009).

CHAPTER 5. DISCUSSION

Selenium is an essential micronutrient. In the modern ocean, uptake by phytoplankton results in the near-complete removal of dissolved Se from marine surface waters, and subsequent export from the photic zone primarily under the form of organically-bound selenide (Cutter and Bruland, 1984; Doblin et al., 2006; Ohlendorf, 1989; Wrench and Measures, 1982). The Se/TOC ratio of modern marine plankton therefore provides a useful reference to which sediment Se/TOC ratios can be compared. The lowest marine plankton Se/TOC values, on the order of $1.8x10^{-6}$ mol/mol, have been reported for Subantarctic Surface Water (SASW) and Subtropical Surface Water (STW) (Sherrard et al., 2004). Cultured phytoplankton have Se/TOC values around $3.2x10^{-6}$ mol/mol, which also appears to be the mean value of Se/TOC found in marine planktonic assemblages (Doblin et al., 2006). Plankton collected in Northern San Francisco Bay has a slightly higher Se/TOC ratio ($5.7x10^{-6}$ mol/mol, Doblin et al., 2006).

For the modern and ancient marine sediments analyzed in this study, the sediment Se/TOC values are either compatible with or greater than the values observed for modern marine plankton (Figure 11). The most depleted Se/TOC ratios are found in the laminated black shales of the New Albany formation, with values at the lower end of the modern plankton range. The Se/TOC values of the Black Sea, Alum Shale and Toarcian OAE samples are close to the average Se/TOC of modern marine phytoplankton. All the remaining sediments and sedimentary rocks are enriched in Se relative to marine plankton, indicating

either selective enrichment processes or additional sources of Se to the sediment. The Se isotopic signatures may potentially help explain the observed variations in the sediment Se/TOC ratios.

Given the large Se isotope fractionations reported in laboratory studies, especially fractionations associated with reductive processes (Figure 1), the range of $\delta^{82/76}$Se values in the sediments and sedimentary rocks analyzed here is surprisingly narrow (Figure 11). In addition, most values fall close to the $\delta^{82/76}$Se value of plankton collected in the oligotrophic Pacific Ocean ($\delta^{82/76}$Se = 0.42‰, this study). This is particularly true for the Black Sea and the Alum Shale Formation, whose samples also have Se/TOC ratios that are indistinguishable from those of modern marine plankton. We therefore tentatively conclude that the dominant source of Se in the sediments from the Black Sea and the Alum Shale Formation is the deposition of marine plankton debris. The deposited Se would then already be in its most reduced form, -II, thereby excluding further fractionation effects due to reduction processes in the sediments.

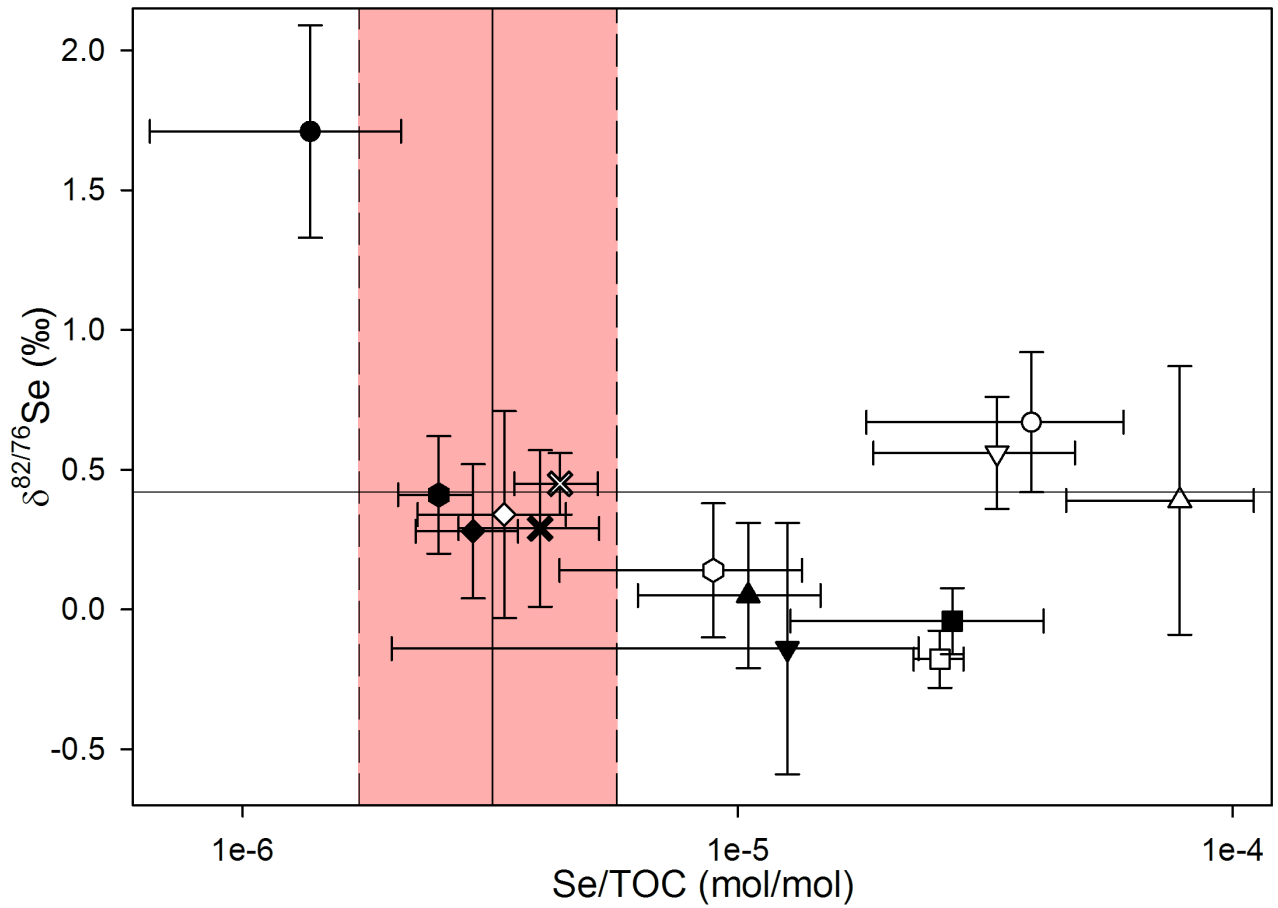

Figure 11 Average Se/TOC ratios versus $\delta^{82/76}$Se. Solid vertical line indicates average Se:C of phytoplankton, (Doblin et al., 2006) dashed vertical lines indicate upper (Doblin et al., 2006) and lower (Sherrard et al., 2004) limit of observed Se:C ratios in phytoplankton. Red shading encompasses Se:C ratios observed in phytoplankton. Solid horizontal line indicates average oligotrophic open Pacific Ocean planktonic $\delta^{82/76}$Se (this study). Symbols: X=Black Sea; circles=New Albany Shale; hexagon=Posidonia Shale; diamond=Alum Shale; square=Arabian Sea; triangle, down=Demerara Rise; triangle, up=Cape Verde Basin. Symbol shading corresponds to the categories used in Figure 4 with the exception of the OAE sites where the before and after OAE data have been combined. Error bars indicate the standard deviation (1σ) of the average values of Se/TOC and $\delta^{82/76}$Se.

The proposed interpretation for the Black Sea and Alum Shale $\delta^{82/76}$Se values implies that the isotopic signatures preserved in the corresponding sediments primarily reflect fractionation accompanying the reductive assimilation of Se by phytoplankton in the surface waters. To our knowledge, there has only been one study in which fractionation during assimilatory Se uptake using a freshwater algae (*Chlamydomonas reinhardtii*). The corresponding fractionations are relatively small (ε=1.65 to 3.90‰, Figure 1). If we assume that fractionation by marine plankton is of similar magnitude, we would expect seawater to have a slightly positive $\delta^{82/76}$Se, on the order of 3±3‰. Unfortunately, no direct measurements of the Se isotopic composition of modern seawater have been performed yet. In addition, there are no data currently available to independently reconstruct ancient seawater Se isotopic composition. Nonetheless, the narrow range of $\delta^{82/76}$Se values in the sediments, shales and mudstones analyzed in this study argues against large seawater $\delta^{82/76}$Se variations over the course of the Phanerozoic. This hypothesis remains to be verified.

Sources of Se to sediments other than marine organic matter include products of continental weathering and submarine volcanism. Weathering on land yields isotopically light alteration products. Extreme Se enrichments in supergene ore deposits have $\delta^{82/76}$Se values as low as -14.2‰ (Wen et al., 2007; Zhu et al., 2008). Typical $\delta^{82/76}$Se values of land-derived materials are likely less negative. Rouxel et al. (2002), for instance, report an average $\delta^{82/76}$Se of -0.42‰ for terrigenous clay samples from the Izu-Bonin-Mariana Margin (ODP Leg 185, Site 1149, Late Pleistocene). This value is probably more representative of continental weathering products delivered to the oceans. Terrigenous Se input may explain the excess Se/TOC ratios and relatively light isotopic signatures of the Arabian Sea sediments (Figure 11). Based on the average $\delta^{82/76}$Se values of terrigenous (-0.42‰) and marine plankton Se (+0.42‰) mentioned above, isotopic balance implies contributions of terrigenous Se on the order of 83 and 73% for cores 464 and 463, respectively. These estimates agree remarkably well with those obtained independently for the same cores by van der Weijden et al. (2006) using Se to aluminum (Al) concentration ratios, and assuming that all Al is of terrigenous origin.

Bottom water oxygenation inferred from biomarkers indicates that the sediments of core 463

were deposited under predominantly anoxic conditions, while core 464 experienced mostly oxic conditions (Sinninghe-Damsté et al., 2002). Bottom water oxygenation varies but little change in Se/TOC and $\delta^{82/76}$Se because the dominant source at both sites is terrigenous. A different trend is seen in the Posidonia Shale sequence where the Se/TOC ratios and isotopic Se composition during the Toarcian OAE shift entirely to the modern planktonic values. During OAE increased deposition of marine organic matter increases relative to the terrigenous input shifting Se/TOC and $\delta^{82/76}$Se values toward modern planktonic values.

In contrast to the Arabian Sea and Posidonia Shale, in the New Albany Shale formation deposition under more reducing water column conditions causes the Se isotopic composition to shift away from the modern planktonic value. In addition to the most positive $\delta^{82/76}$Se values, the laminated New Albany shale layers also exhibit the lowest Se/TOC ratios (Figure 11). One possible explanation is that the Se signatures in the laminated shales reflect high primary productivity under extreme water column Se limitation. The reduced availability of Se would not only lead to the burial of Se-depleted organic matter, but also decrease the extent of fractionation during assimilatory Se uptake. The black shale isotopic compositions would then yield a minimum estimate of $\delta^{82/76}$Se of Late Devonian-Early Mississippian seawater of 1.7±0.5‰.

Lower primary productivity during deposition of the bioturbated shales of the New Albany Shale sequence (Ingall et al., 1993) would alleviate Se limitation and deliver isotopically lighter organically-bound Se to the seafloor. The high Se/TOC ratios could be accounted for by additional Se deposition, for example, as selenium sorbed to settling mineral matter. Under oxic conditions in the water column, ferric iron oxyhydroxides are expected to be an important carrier phase for Se oxyanions. Due to small fractionations associated with Se adsorption to ferric iron oxyhydroxides ($\varepsilon \approx 0.8$‰, Johnson and Bullen, 2004; Johnson et al., 1999) the sorbed Se would be slightly lighter than seawater. The net effect would be sediment $\delta^{82/76}$Se values intermediate between seawater and plankton, as observed in Figure 11.

Increased volcanism may have played a major role in triggering OAE2 (Adams et al., 2010; Jenkyns, 2010; Kerr, 1998; Schlanger et al., 1987; Schlanger et al., 1981; Turgeon and Creaser, 2008).

Elevated levels of trace elements have been cited as evidence for intense volcanic activity (Adams et al., 2010; Brumsack, 1986; Hild and Brumsack, 1998; Snow et al., 2005; Turgeon and Creaser, 2008). Volcanogenic Se input could thus explain the high Se/TOC ratios in the Demerara Rise and Cape Verde Basin sediments (Figure 11). Volcanic activity principally releases Se as nano-particulate elemental selenium and volatile selenium compounds (Suzuoki, 1964). The former could be directly incorporated as Se(0) in marine sediments, while the latter would increase the availability of Se in the water column, which may cause luxury Se uptake by phytoplankton (Baines and Fisher, 2001; Vandermeulen and Foda, 1988). Excess Se may also have been removed from the water column as Se oxyanions sorbed to settling mineral matter, further enriching the sediments in Se.

Ocean basalts have isotopic compositions very near that of modern marine plankton ($\delta^{82/76}Se$ = 0.25‰; Rouxel et al., 2004). Most likely, the volatile and nano-particulate Se associated with marine volcanism have isotopic compositions close to the basaltic value. Hence, sediment $\delta^{82/76}Se$ records should not differentiate between marine planktonic and volcanogenic Se sources. The average $\delta^{82/76}Se$ values of the sediments deposited during OAE2 are distinctly lower than for the sediments deposited before and after the event (Figure 11). We attribute this to the microbial or chemical reduction of excess Se(VI) and Se(IV) oxyanions within the euxinic water column of OAE2. Both biotic and abiotic reduction would result in the production of isotopically light particulate Se(0) or FeSe, which would settle to the seafloor. During the less reducing conditions prevailing before and after OAE2, however, sorbed Se oxyanions would be delivered to the sediments. Subsequent Se reduction would occur in the semi-closed sediment system, hence producing isotopically heavier reduced Se than during the OAE.

The biogeochemical processes that are thought to control marine sedimentary Se records are summarized in Figure 12. Admittedly, many of the proposed interpretations of the Se/TOC ratios and $\delta^{82/76}Se$ values of the sediments and sedimentary rocks analyzed in this study are speculative. Their verification will require a more complete characterization of the chemical speciation and isotopic composition of the key pools and fluxes of the marine Se cycle, as well as a better understanding of the processes that affect the oceanic cycling and early diagenetic fate of Se.

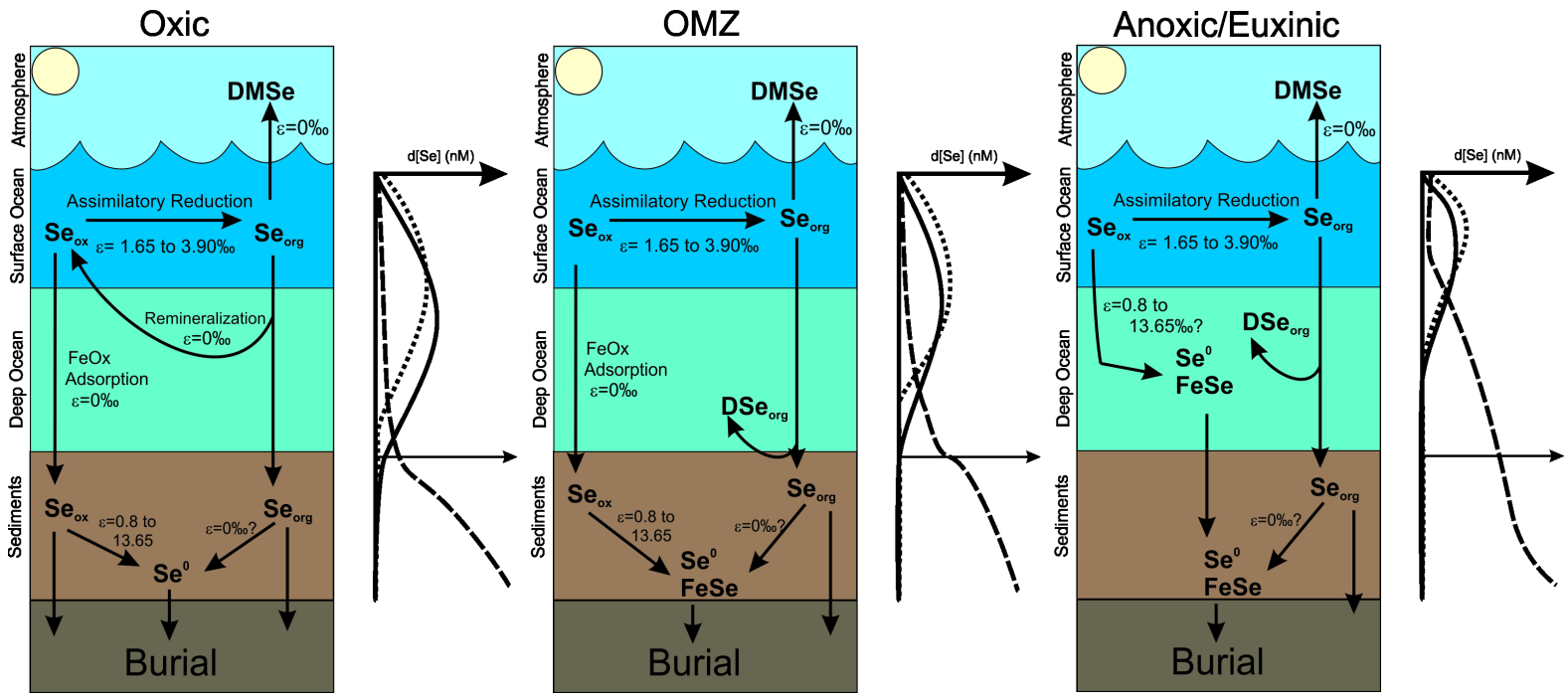

Figure 12 Proposed selenium cycling under various water column redox conditions. Depth profiles of dissolved selenium species concentrations are shown schematically next to each ocean panel: dotted line indicates Se(VI), solid line indicates Se(IV), long dash indicates DSe_{org}. On the panels, Se_{ox} includes Se(VI) and Se(IV), DSe_{org} stands for dissolved organic selenium.

CHAPTER 6. CONCLUSIONS

This study provides a first assessment of the paleooceanographic proxy potential of selenium records in fine-grained marine sediments and sedimentary rocks. The Se concentrations and Se/TOC ratios show significant variability, which reflect changes over time of the sources, water column availability and sedimentary sinks of Se. The variations in $\delta^{82/76}$Se, albeit small, further constrain the interpretations of the cycling of Se under different oceanographic regimes. For example, we propose that the negative $\delta^{82/76}$Se excursion observed for shales deposited during OAE2 are due to reduction of Se(VI, IV) oxyanions in the euxinic water column and their subsequent burial as elemental Se and iron-bound selenide. A similar isotopic signature is not observed in modern sediments deposited under euxinic bottom waters in the Black Sea, presumably because of a much lower water column availability of Se. This would explain why the Black Sea sediments exhibit Se/TOC ratios close to those of marine plankton, while the OAE2 shales are enriched in Se relative to marine plankton.

Because of the large diversity of oxidation states and geochemical forms of Se, bulk sediment concentrations and isotopic signatures only offer a partial window into past depositional conditions and biogeochemical processes. Quantitative information on the speciation of Se in marine sediments and sedimentary rocks would significantly strengthen the selenium proxy, especially if the chemical differentiation of the sedimentary pools of Se is coupled to their isotopic fingerprinting. Equally important, however, is to fully characterize all the end-member sources that contribute Se to marine sediments. The existing data sets on Se contents, speciation and isotopic ratios of marine and terrestrial organic matter, continental weathering products, river run-off, and volcanic plus hydrothermal inputs are limited at best. Similarly, there remain many gaps in our understanding of the isotopic fractionations associated with key processes in the marine Se cycle.

The results presented in this study should be useful in prioritizing further research efforts in the field of selenium biogeochemistry and isotope geochemistry. Even with the current state of knowledge, however, sedimentary Se records may play a useful role in paleooceanographic reconstructions, as part of a multi-proxy approach.

REFERENCES

Adams, D.D., Hurtgen, M.T., Sageman, B.B., 2010. Volcanic triggering of a biogeochemical cascade during Oceanic Anoxic Event 2. Nature Geosci 3, 201-204. 10.1038/ngeo743

Ahlberg, P., Axheimer, N., Babcock, L.E., Eriksson, M.E., Schmitz, B., Terfelt, F., 2009. Cambrian high-resolution biostratigraphy and carbon isotope chemostratigraphy in Scania, Sweden: first record of the SPICE and DICE excursions in Scandinavia. Lethaia 42, 2-16. 10.1111/j.1502-3931.2008.00127.x

Amouroux, D., Donard, O.F.X., 1996. Maritime Emission of Selenium to the Atmosphere in Eastern Mediterranean seas. Geophys. Res. Lett. 23. 10.1029/96gl01271

Amouroux, D., Liss, P.S., Tessier, E., Hamren-Larsson, M., Donard, O.F.X., 2001. Role of oceans as biogenic sources of selenium. Earth and Planetary Science Letters 189, 277-283. doi: DOI: 10.1016/S0012-821X(01)00370-3

Ansede, J.H., Yoch, D.C., 1997. Comparison of selenium and sulfur volatilization by dimethylsulfoniopropionate lyase (DMSP) in two marine bacteria and estuarine sediments. FEMS Microbiology Ecology 23, 315-324. 10.1111/j.1574-6941.1997.tb00412.x

Arnold, G.L., Anbar, A.D., Barling, J., Lyons, T.W., 2004. Molybdenum Isotope Evidence for Widespread Anoxia in Mid-Proterozoic Oceans. Science 304, 87-90. 10.1126/science.1091785

Arthur, M.A., Schlanger, S.O., Jenkyns, H.C., 1987. The Cenomanian-Turonian Oceanic Anoxic Event, II. Palaeoceanographic controls on organic-matter production and preservation. Geological Society, London, Special Publications 26, 401-420. 10.1144/gsl.sp.1987.026.01.25

Atkinson, R., Aschmann, S.M., Hasegawa, D., Thompson-Eagle, E.T., Frankenberger, W.T., 1990. Kinetics of the atmospherically important reactions of dimethyl selenide. Environmental Science & Technology 24, 1326-1332. 10.1021/es00079a005

Baines, S.B., Fisher, N.S., 2001. Interspecific differences in the bioconcentration of selenite by phytoplankton and their ecological implications. Marine Ecology Progress Series 213, 1-12. 10.3354/meps213001

Baines, S.B., Fisher, N.S., Doblin, M.A., Cutter, Gregory A., 2001. Uptake of dissolved organic selenides by marine phytoplankton. Limnology and Oceanography 46, 1936-1944.

Balistrieri, L.S., Chao, T.T., 1987. Selenium Adsorption by Goethite. Soil Sci Soc Am J 51, 1145-1151.

Beier, J.A., Hayes, J.M., 1989. Geochemical and isotopic evidence for paleoredox conditions during deposition of the Devonian-Mississippian New Albany Shale, southern Indiana. Geological Society of America Bulletin 101, 774-782. 10.1130/0016-7606(1989)101<0774:gaiefp>2.3.co;2

Böck, A., Forchhammer, K., Heider, J., Leinfelder, W., Sawers, G., Veprek, B., Zinoni, F., 1991. Selenocysteine: the 21st amino acid. Molecular Microbiology 5, 515-520. 10.1111/j.1365-2958.1991.tb00722.x

Breynaert, E., Bruggeman, C., Maes, A., 2008. XANES-EXAFS Analysis of Se Solid -Phase Reaction Products Formed upon Contacting Se(IV) with FeS_2 and FeS. Environmental Science & Technology 42, 3595-3601. 10.1021/es071370r

Bruggeman, C., Maes, A., Vancluysen, J., 2007. The interaction of dissolved Boom Clay and Gorleben humic substances with selenium oxyanions (selenite and selenate). Applied Geochemistry 22, 1371-1379. DOI: 10.1016/j.apgeochem.2007.03.027

Bruggeman, C., Maes, A., Vancluysen, J., Vandemussele, P., 2005. Selenite reduction in Boom clay: Effect of FeS_2, clay minerals and dissolved organic matter. Environmental Pollution 137, 209-221. 10.1016/j.envpol.2005.02.010

Brumsack, H.-J., 1991. Inorganic geochemistry of the German 'Posidonia Shale': palaeoenvironmental consequences. Geological Society, London, Special Publications 58, 353-362. 10.1144/gsl.sp.1991.058.01.22

Brumsack, H.J., 1986. The inorganic geochemistry of Cretaceous black shales (DSDP Leg 41) in comparison to modern upwelling sediments from the Gulf of California. Geological Society, London, Special Publications 21, 447-462. 10.1144/gsl.sp.1986.021.01.30

Calvert, S.E., Bustin, R.M., Ingall, E.D., 1996. Influence of water column anoxia and sediment supply on the burial and preservation of organic carbon in marine shales. Geochimica et Cosmochimica Acta 60, 1577-1593. 10.1016/0016-7037(96)00041-5

Calvert, S.E., Pedersen, T.F., Naidu, P.D., von Stackelberg, U., 1995. On the organic carbon maximum on the continental slope of the eastern Arabian Sea. Journal of Marine Research 53, 269-296. 10.1357/0022240953213232

Canfield, D.E., 2001. Biogeochemistry of sulfur isotopes, in: Valley, J.W., Cole, D.R. (Eds.), Stable Isotope Geochemistry. Mineralogical Society of America, Washington, DC., pp. 607-636.

Canfield, D.E., Lyons, T.W., Raiswell, R., 1996. A model for iron deposition to euxinic Black Sea sediments. Am J Sci 296, 818-834. 10.2475/ajs.296.7.818

Canfield, D.E., Olesen, C.A., Cox, R.P., 2006. Temperature and its control of isotope fractionation by a sulfate-reducing bacterium. Geochimica Et Cosmochimica Acta 70, 548-561. 10.1016/j.gca.2005.10.028

Challenger, F., North, H.E., 1934. The production of organo-metalloidal compounds by micro-organisms. Part II. Dimethyl selenide. Journal of Chemical Society, 68-71.

Charlet, L., Scheinost, A.C., Tournassat, C., Greneche, J.M., Gehin, A., Fernandez-Marti'nez, A., Coudert, S., Tisserand, D., Brendle, J., 2007. Electron transfer at the mineral/water interface: Selenium reduction by ferrous iron sorbed on clay. Geochimica et Cosmochimica Acta 71, 5731-5749. 10.1016/j.gca.2007.08.024

Chasteen, T.G., 1998. Volatile Chemical Species of Selenium, in: Frankenberger Jr., E., R.A. (Ed.), Environmental Chemistry of Selenium. Marcel Dekker, New York, pp. 589-612.

Chau, Y.K., Wong, P.T.S., Silverberg, B.A., Luxon, P.L., Bengert, G.A., 1976. Methylation of Selenium in the Aquatic Environment. Science 192, 1130-1131. 10.1126/science.192.4244.1130

Chen, Y.-W., Zhou, X.-L., Tong, J., Truong, Y., Belzile, N., 2005. Photochemical behavior of inorganic and organic selenium compounds in various aqueous solutions. Analytica Chimica Acta 545, 149-157. 10.1016/j.aca.2005.03.033

Clark, S.K., 2007. Selenium stable isotope ratios in wetlands: Insights into biogeochemical cycling and how a diffusive barrier affects the measured fractionation factor. University of Illinois at Urbana-Champaign, Geology Departement, PhD Thesis, 135.

Clark, S.K., Johnson, T.M., 2008. Effective Isotopic Fractionation Factors for Solute Removal by Reactive Sediments: A Laboratory Microcosm and Slurry Study. Environmental Science & Technology 42, 7850-7855. 10.1021/es801814v

Cluff, R.M., 1980. Paleoenvironment of the New Albany Shale Group (Devonian-Mississippian) of Illinois. Journal of Sedimentary Research 50, 767-780.

Cutter, G.A., 1982. Selenium in Reducing Waters. Science 217, 829-831.

Cutter, G.A., Bruland, K.W., 1984. The marine biogeochemistry of selenium: A re-evaluation. Limnology and Oceanography 29, 1179-1192.

Cutter, G.A., Cutter, L.S., 1995. Behavior of dissolved antimony, arsenic, and selenium in the Atlantic Ocean. Marine Chemistry 49, 295-306. 10.1016/0304-4203(95)00019-N

DeMoll-Decker, H., Macy, J.M., 1993. The periplasmic nitrite reductase of *Thauera selenatis* may catalyze the reduction of selenite to elemental selenium. Archives of Microbiology 160, 241-247. 10.1007/BF00249131

DiChristina, T.J., Fredrickson, J.K., Zachara, J.M., 2005. Enzymology of Electron Transport: Energy Generation With Geochemical Consequences. Reviews in Mineralogy and Geochemistry 59, 27-52. 10.2138/rmg.2005.59.3

Doblin, M.A., Baines, S.B., Cutter, L.S., Cutter, G.A., 2006. Sources and biogeochemical cycling of particulate selenium in the San Francisco Bay estuary. Estuarine, Coastal and Shelf Science 67, 681-694.

Dowdle, P.R., Oremland, R.S., 1998. Microbial oxidation of elemental selenium in soil slurries and bacterial cultures. Environmental Science & Technology 32, 3749-3755. 10.1021/es970940s

Ellis, A.S., Johnson, T.M., Herbel, M.J., Bullen, T.D., 2003. Stable isotope fractionation of selenium by natural microbial consortia. Chemical Geology 195, 119-129. 10.1016/S0009-2541(02)00391-1

Erbacher, J., Friedrich, O., Wilson, P.A., Birch, H., Mutterlose, J., 2005. Stable organic carbon isotope stratigraphy across Oceanic Anoxic Event 2 of Demerara Rise, western tropical Atlantic. Geochem. Geophys. Geosyst. 6, Q06010. 10.1029/2004gc000850

Fisher, I.S.J., Hudson, J.D., 1987. Pyrite formation in Jurassic shales of contrasting biofacies. Geological Society, London, Special Publications 26, 69-78. 10.1144/gsl.sp.1987.026.01.04

Gamboa-Lewis, B.A., 1976. Selenium in Biological Systems, and Pathways for its Volitalization in Higher Plants, in: Nriagu, J.O. (Ed.), Environmental Biogeochemistry. Ann Arbor Science, Ann Arbor, pp. 389-409.

Gill, B.C., Lyons, T.W., Young, S.A., Kump, L.R., Knoll, A.H., Saltzman, M.R., 2011. Geochemical evidence for widespread euxinia in the Later Cambrian ocean. Nature 469, 80-83. 10.1038/nature09700

Gladyshev, V.N., Kryukov, G.V., 2001. Evolution of selenocysteine-containing proteins: Significance of identification and functional characterization of selenoproteins. Biofactors 14, 87.

Glumac, B., Walker, K.R., 1998. A Late Cambrian positive carbon-isotope excursion in the Southern Appalachians; relation to biostratigraphy, sequence stratigraphy, environments of deposition, and diagenesis. Journal of Sedimentary Research 68, 1212-1222.

Gralnick, J.A., Newman, D.K., 2007. Extracellular respiration. Molecular Microbiology 65, 1-11. 10.1111/j.1365-2958.2007.05778.x

Habicht, K.S., Gade, M., Thamdrup, B., Berg, P., Canfield, D.E., 2002. Calibration of Sulfate Levels in the Archean Ocean. Science 298, 2372-2374. 10.1126/science.1078265

Hagiwara, Y., 2000. Selenium isotope ratios in marine sediments and algae. A reconnaissance study. University of Illinois at Urbana-Champaign, Geology, MS Thesis.

Hayes, K.F., Roe, A.L., Brown, G.E., JR., Hodgson, K.O., Leckie, J.O., Parks, G.A., 1987. In Situ X-ray Absorption Study of Surface Complexes: Selenium Oxyanions on α-FeOOH. Science 238, 783-786. 10.1126/science.238.4828.783

Herbel, M.J., Blum, J.S., Oremland, R.S., Borglin, S.E., 2003. Reduction of elemental selenium to selenide: Experiments with anoxic sediments and bacteria that respire Se-oxyanions. Geomicrobiology Journal 20, 587-602. 10.1080/713851163

Herbel, M.J., Johnson, T.M., Oremland, R.S., Bullen, T.D., 2000. Fractionation of selenium isotopes during bacterial respiratory reduction of selenium oxyanions. Geochimica Et Cosmochimica Acta 64, 3701-3709. 10.1016/S0016-7037(00)00456-7

Herbel, M.J., Johnson, T.M., Tanji, K.K., Gao, S.D., Bullen, T.D., 2002. Selenium stable isotope ratios in California agricultural drainage water management systems. Journal of Environmental Quality 31, 1146-1156.

Herbin, J.P., Montadert, L., Muller, C., Gomez, R., Thurow, J., Wiedmann, J., 1986. Organic-rich sedimentation at the Cenomanian-Turonian boundary in oceanic and coastal basins in the North Atlantic and Tethys. Geological Society, London, Special Publications 21, 389-422. 10.1144/gsl.sp.1986.021.01.28

Hild, E., Brumsack, H.J., 1998. Major and minor element geochemistry of Lower Aptian sediments from the NW German Basin (core Hohenegglesen KB 40). Cretaceous Research 19, 615-633. DOI: 10.1006/cres.1998.0122

Hockin, S.L., Gadd, G.M., 2003. Linked redox precipitation of sulfur and selenium under anaerobic conditions by sulfate-reducing bacterial biofilms. Applied and Environmental Microbiology 69, 7063-7072. 10.1128/AEM.69.12.7063-7072.2003

Hockin, S.L., Gadd, G.M., 2006. Removal of selenate from sulfate-containing media by sulfate-reducing bacterial biofilms. Environmental Microbiology 8, 816-826. 10.1111/j.1462-2920.2005.00967.x

Hoek, J., Reysenbach, A.-L., Habicht, K.S., Canfield, D.E., 2006. Effect of hydrogen limitation and temperature on the fractionation of sulfur isotopes by a deep-sea hydrothermal vent sulfate-reducing bacterium. Geochimica et Cosmochimica Acta: A Special Issue Dedicated to Robert A. Berner 70, 5831-5841. 10.1016/j.gca.2006.07.031

Howard III, J.H., 1977. Geochemistry of selenium: formation of ferroselite and selenium behavior in the vicinity of oxidizing sulfide and uranium deposits. Geochimica et Cosmochimica Acta 41, 1665-1678.

Ingall, E.D., Bustin, R.M., Van Cappellen, P., 1993. Influence of water column anoxia on the burial and preservation of carbon and phosphorus in marine shales. Geochimica et Cosmochimica Acta 57, 303-316. 10.1016/0016-7037(93)90433-W

Jenkyns, H.C., 2010. Geochemistry of oceanic anoxic events. Geochem. Geophys. Geosyst. 11, Q03004. 10.1029/2009gc002788

Johnson, T.M., 2004. A review of mass-dependent fractionation of selenium isotopes and implications for other heavy stable isotopes. Chemical Geology 204, 201-214. 10.1016/j.chemgeo.2003.11.015

Johnson, T.M., Bullen, T.D., 2003. Selenium isotope fractionation during reduction by Fe(II)-Fe(III) hydroxide-sulfate (green rust). Geochimica et Cosmochimica Acta 67, 413-419. 10.1016/S0016-7037(02)01137-7

Johnson, T.M., Bullen, T.D., 2004. Mass-Dependent Fractionation of Selenium and Chromium Isotopes in Low-Temperature Environments. Reviews in Mineralogy and Geochemistry 55, 289-317. 10.2138/gsrmg.55.1.289

Johnson, T.M., Herbel, M.J., Bullen, T.D., Zawislanski, P.T., 1999. Selenium isotope ratios as indicators of selenium sources and oxyanion reduction. Geochimica et Cosmochimica Acta 63, 2775-2783. 10.1016/S0016-7037(99)00279-3

Kenward, P.A., Fowle, D.A., Yee, N., 2006. Microbial Selenate Sorption and Reduction in Nutrient Limited Systems. Environmental Science & Technology 40, 3782-3786. 10.1021/es052210n

Kerr, A.C., 1998. Oceanic plateau formation: a cause of mass extinction and black shale deposition around the Cenomanian-Turonian boundary? Journal of the Geological Society 155, 619-626. 10.1144/gsjgs.155.4.0619

Kessi, J., Hanselmann, K.W., 2004. Similarities between the Abiotic Reduction of Selenite with Glutathione and the Dissimilatory Reaction Mediated by *Rhodospirillum rubrum* and *Escherichia coli*. Journal of Biological Chemistry 279, 50662-50669. 10.1074/jbc.M405887200

Kikuchi, E., Sakamoto, H., 2000. Kinetics of the Reduction Reaction of Selenate Ions by TiO[sub 2] Photocatalyst. Journal of The Electrochemical Society 147, 4589-4593.

Krouse, H.R., Thode, H.G., 1962. Thermodynamic properties and geochemistry of isotopic compounds of selenium. Canadian Journal of Chemistry 40, 367-375. 10.1139/v62-055

Kuypers, M.M.M., Pancost, R.D., Nijenhuis, I.A., Sinninghe Damsté, J.S., 2002. Enhanced productivity led to increased organic carbon burial in the euxinic North Atlantic basin during the late Cenomanian oceanic anoxic event. Paleoceanography 17, 1051. 10.1029/2000pa000569

Lide, D.R., 2006. CRC Handbook of Chemistry and Physics, 87 ed. CRC Press, Boca Raton.

Lovley, D.R., 2006. Bug juice: harvesting electricity with microorganisms. Nature Reviews Microbiology 4, 497-508. 10.1038/nrmicro1442

Lovley, D.R., Phillips, E.J.P., 1994. Novel Processes for Anaerobic Sulfate Production from Elemental Sulfur by Sulfate-Reducing Bacteria. Applied Environmental Microbiology 60, 2394-2399.

Lyons, T.W., 1991. Upper Holocene sediments of the Black Sea: Summary of Leg 4 Box Cores (1988 Black Sea Oceanographic Expedition), in: Izdar, E., Murray, J.W. (Eds.), Black Sea Oceanography. Kluwer Academic Publisher, pp. 401-441.

Lyons, T.W., Berner, R.A., Anderson, R.F., 1993. Evidence for large pre-industrial perturbations of the Black Sea chemocline. Nature 365, 538-540. 10.1038/365538a0

Lyons, T.W., Kashgarian, M., 2005. Paradigm lost, paradigm found-The Black Sea-black shale connection as viewed from the anoxic basin margin. Oceanography 18, 86-99.

Mayland, H.F., 1994. Selenium in Plant and Animal Nutrition, in: Frankenberger Jr., W.T., Benson, S. (Eds.), Selenium in the Environment. Marcel-Dekker, New York, pp. 29-47.

Measures, C.I., Burton, J.D., 1980a. Gas chromatographic method for the determination of selenite and total selenium in sea water. Analytica Chimica Acta 120, 177-186.

Measures, C.I., Burton, J.D., 1980b. The vertical distribution and oxidation states of dissolved selenium in the northeast Atlantic Ocean and their relationship to biological processes. Earth and Planetary Science Letters 46, 385-396.

Measures, C.I., Grant, B.C., Mangum, B.J., Edmond, J.M., 1983. The Relationship of the distribution of dissolved selenium IV and VI in three oceans to the physical and biological process, in: Wong, C.S., Boyle, E., Bruland, K.W., Burton, J.D., Goldberg, E.D. (Ed.), Trace Metals In Sea water. Plenum Press, New York.

Milne, J.B., 1998. The Uptake and Metablolism of Inorganic Selenium Species, in: Frankenberger Jr., W.T., Engberg, R.A. (Ed.), Environmental Chemistry of Selenium. Marcel Dekker, New York, pp. 459-477.

Mitchell, K., Heyer, A., Canfield, D.E., Hoek, J., Habicht, K.S., 2009. Temperature effect on the sulfur isotope fractionation during sulfate reduction by two strains of the hyperthermophilic *Archaeoglobus fulgidus*. Environmental Microbiology 11, 2998-3006. 10.1111/j.1462-2920.2009.02002.x

Morrison, J.M., Codispoti, L.A., Smith, S.L., Wishner, K., Flagg, C., Gardner, W.D., Gaurin, S., Naqvi, S.W.A., Manghnani, V., Prosperie, L., Gundersen, J.S., 1999. The oxygen minimum zone in the Arabian Sea during 1995. Deep Sea Research Part II: Topical Studies in Oceanography 46, 1903-1931. Doi: 10.1016/s0967-0645(99)00048-x

Mosher, B.W., Duce, R.A., 1987. A Global Atmospheric selenium budget. Journal of Geophysical Research 92, 13,289-213,298. 10.1029/JD092iD11p13289

Myneni, S.C.B., Tokunaga, T.K., Brown, G.E., Jr., 1997. Abiotic Selenium Redox Transformations in the Presence of Fe(II,III) Oxides. Science 278, 1106-1109. 10.1126/science.278.5340.1106

Neal, R.H., Sposito, G., 1989. Selenate Adsorption on Alluvial Soils. Soil Sci Soc Am J 53, 70-74.

Neal, R.H., Sposito, G., Holtzclaw, K.M., Traina, S.J., 1987. Selenite Adsorption on Alluvial Soils: I. Soil Composition and pH Effects. Soil Sci Soc Am J 51, 1161-1165.

Newport, P.J., Nedwell, D.B., 1988. The mechanisms of inhibition of Desulfovibrio and Desulfotomaculum. Journal of Applied Bacteriology 65, 419-423.

Nguyen, V.N.H., Beydoun, D., Amal, R., 2005. Photocatalytic reduction of selenite and selenate using TiO_2 photocatalyst. Journal of Photochemistry and Photobiology A: Chemistry 171, 113-120. 10.1016/j.jphotochem.2004.09.015

Ohlendorf, H.M., 1989. Bioaccumulation and Effects of Selenium on Wildlife, in: Jacobs, L.W. (Ed.), Selenium in Agriculture and the Environment. American Society of Agronomy, Madison, pp. 133-177.

Oldfield, J.E., 2002. Selenium World Atlas. Selenium-Tellurium Development Association.

Oram, L.L., Strawn, D.G., Marcus, M.A., Fakra, S.C., Möller, G., 2008. Macro- and Microscale Investigation of Selenium Speciation in Blackfoot River, Idaho Sediments. Environmental Science & Technology 42, 6830-6836. 10.1021/es7032229

Oremland, R.S., 1991. In situ bacterial selenate reduction in the agricultural drainage systems of western Nevada. Appl. Environ. Microbiol. 57, 615-617.

Oremland, R.S., 1994. Biogeochemical Transformations of Selenium in Anoxic Environments, in:

Frankenberger Jr., W.T., Benson, S. (Ed.), Selenium in the Environment. Marcel Dekker, New York, pp. 389-419.

Oremland, R.S., Blum, J.S., Culbertson, C.W., Visscher, P.T., Miller, L.G., Dowdle, P.R., Strohmaier, F.E., 1994. Isolation, Growth, and Metabolism of an Obligately Anaerobic, Selenate-Respiring Bacterium, Strain Ses-3. Applied and Environmental Microbiology 60, 3011-3019.

Oremland, R.S., Hollibaugh, J.T., Maest, A.S., Presser, T.S., Miller, L.G., Culbertson, C.W., 1989. Selenate Reduction to Elemental Selenium by Anaerobic-Bacteria in Sediments and Culture - Biogeochemical Significance of a Novel, Sulfate-Independent Respiration. Applied and Environmental Microbiology 55, 2333-2343.

Oremland, R.S., Steinberg, N.A., Maest, A.S., Miller, L.G., Holllbaugh, J.T., 1990. Measurement of in Situ Rates of Selenate Removal by Dissimilatory Bacterial Reduction in Sediments. Enviromental Science and Technology 24, 1157-1164.

Pearce, C.I., Coker, V.S., Charnock, J.M., Pattrick, R.A.D., Mosselmans, J.F.W., Law, N., Beveridge, T.J., Lloyd, J.R., 2008. Microbial manufacture of chalcogenide-based nanoparticles via the reduction of selenite using *Veillonella atypica*: an in situ EXAFS study. Nanotechnology 19, 155603. 10.1088/0957-4484/19/15/155603

Plant, J.A., Kinniburgh, D.G., Smedley, P.L., Fordyce, F.M., Klinck, B.A., Heinrich, D.H., Karl, K.T., 2003. Arsenic and Selenium. Treatise on Geochemistry 9, 17-66. 10.1088/0957-4484/19/15/155603

Raiswell, R., Canfield, D.E., 1998. Sources of iron for pyrite formation in marine sediments. American Journal of Science 298, 219-245.

Rashid, K., Krouse, H.R., 1985. Selenium isotopic fractionation during SeO_3^{2-} reduction to Se^0 and H_2Se. Canadian Journal of Chemistry 63, 3195-3199. 10.1139/v85-528

Reamer, D.C., Zoller, W.H., 1980. Selenium Biomethylation Products from Soil and Sewage Sludge. Science 208, 500-502. 10.1126/science.208.4443.500

Rees, C.E., 1973. A steady-state model for sulphur isotope fractionation in bacterial reduction processes. Geochimica et Cosmochimica Acta 37, 1141-1162. 10.1016/0016-7037(73)90052-5

Rees, C.E., Thode, H.G., 1966. Selenium isotope effects in the reduction of sodium selenite and of sodium selenate. Canadian Journal of Chemistry 44, 419-427. 10.1139/v66-057

Reichart, G.J., den Dulk, M., Visser, H.J., van der Weijden, C.H., Zachariasse, W.J., 1997. A 225 kyr record of dust supply, paleoproductivity and the oxygen minimum zone from the Murray Ridge (northern

Arabian Sea). Palaeogeography, Palaeoclimatology, Palaeoecology 134, 149-169. Doi: 10.1016/s0031-0182(97)00071-0

Reichart, G.J., Lourens, L.J., Zachariasse, e.J., 1998. Temporal Variability in the Northern Arabian Sea Oxygen Minimum Zone (OMZ) during the Last 225,000 Years. Paleoceanography 13, 607-621. 10.1029/98pa02203

Rickard, D., 2006. The solubility of FeS. Geochimica et Cosmochimica Acta 70, 5779-5789.

Röhl, H.-J., Schmid-Röhl, A., Oschmann, W., Frimmel, A., Schwark, L., 2001. The Posidonia Shale (Lower Toarcian) of SW-Germany: an oxygen-depleted ecosystem controlled by sea level and palaeoclimate. Palaeogeography, Palaeoclimatology, Palaeoecology 165, 27-52. 10.1016/S0031-0182(00)00152-8

Rouxel, O., Fouquet, Y., Ludden, J.N., 2004. Subsurface processes at the lucky strike hydrothermal field, Mid-Atlantic ridge: evidence from sulfur, selenium, and iron isotopes. Geochimica et Cosmochimica Acta 68, 2295-2311. 10.1016/j.gca.2003.11.029

Rouxel, O., Ludden, J., Carignan, J., Marin, L., Fouquet, Y., 2002. Natural variations of Se isotopic composition determined by hydride generation multiple collector inductively coupled plasma mass spectrometry. Geochimica et Cosmochimica Acta 66, 3191-3199. 10.1016/S0016-7037(02)00918-3

Rue, E.L., Smith, G.J., Cutter, G.A., Bruland, K.W., 1997. The response of trace element redox couples to suboxic conditions in the water column. Deep Sea Research Part I: Oceanographic Research Papers 44, 113-134. 10.1016/s0967-0637(96)00088-x

Saltzman, M.R., Runnegar, B., Lohmann, K.C., 1998. Carbon isotope stratigraphy of Upper Cambrian (Steptoean Stage) sequences of the eastern Great Basin: Record of a global oceanographic event. Geological Society of America Bulletin 110, 285-297. 10.1130/0016-7606(1998)110<0285:cisouc>2.3.co;2

Sarathchandra, S., Watkinson, J., 1981. Oxidation of elemental selenium to selenite by *Bacillus megaterium*. Science 211, 600-601. 10.1126/science.6779378

Schauble, E.A., 2004. Applying Stable Isotope Fractionation Theory to New Systems. Reviews in Mineralogy and Geochemistry 55, 65-111.

Scheinost, A.C., Charlet, L., 2008. Selenite Reduction by Mackinawite, Magnetite and Siderite: XAS Characterization of Nanosized Redox Products. Environmental Science & Technology 42, 1984-1989. 10.1021/es071573f

Schlanger, S.O., Arthur, M.A., Jenkyns, H.C., Scholle, P.A., 1987. The Cenomanian-Turonian Oceanic Anoxic Event, I. Stratigraphy and distribution of organic carbon-rich beds and the marine $\delta^{13}C$ excursion. Geological Society, London, Special Publications 26, 371-399. 10.1144/gsl.sp.1987.026.01.24

Schlanger, S.O., Jenkyns, H.C., 1976. Cretaceous oceanic anoxic events: causes and consequences. Geologie en mijnbouw 55, 179-184.

Schlanger, S.O., Jenkyns, H.C., Premoli-Silva, I., 1981. Volcanism and vertical tectonics in the Pacific Basin related to global Cretaceous transgressions. Earth and Planetary Science Letters 52, 435-449. Doi: 10.1016/0012-821x(81)90196-5

Schmid-Röhl, A., Röhl, H.-J., Oschmann, W., Frimmel, A., Schwark, L., 2002. Palaeoenvironmental reconstruction of Lower Toarcian epicontinental black shales (Posidonia Shale, SW Germany): global versus regional control. Geobios 35, 13-20. Doi: 10.1016/s0016-6995(02)00005-0

Schroder, I., Rech, S., Krafft, T., Macy, J.M., 1997. Purification and Characterization of the Selenate Reductase from Thauera selenatis. Journal of Biological Chemistry 272, 23765-23768. 10.1074/jbc.272.38.23765

Sherrard, J.C., Hunter, K.A., Boyd, P.W., 2004. Selenium speciation in subantarctic and subtropical waters east of New Zealand: trends and temporal variations. Deep Sea Research Part I: Oceanographic Research Papers 51, 491-506.

Sinninghe-Damsté, J.S., Rijpstra, W.I.C., Reichart, G.J., 2002. The influence of oxic degradation on the sedimentary biomarker record II. Evidence from Arabian Sea sediments. Geochimica et Cosmochimica Acta 66, 2737-2754. Doi: 10.1016/s0016-7037(02)00865-7

Sinninghe Damsté, J.S., Wakeham, S.G., Kohnen, M.E.L., Hayes, J.M., de Leeuw, J.W., 1993. A 6,000-year sedimentary molecular record of chemocline excursions in the Black Sea. Nature 362, 827-829.

Snow, L.J., Duncan, R.A., Bralower, T.J., 2005. Trace element abundances in the Rock Canyon Anticline, Pueblo, Colorado, marine sedimentary section and their relationship to Caribbean plateau construction and oxygen anoxic event 2. Paleoceanography 20, PA3005. 10.1029/2004pa001093

Stadtman, T.C., 1990. Selenium Biochemistry. Annual Review of Biochemistry 59, 111-127. doi:10.1146/annurev.bi.59.070190.000551

Stams, A.J.M., de Bok, Frank A. M., Plugge, Caroline M. , van Eekert, Miriam H. A., Dolfing, Jan, Schraa,Gosse, 2006. Exocellular electron transfer in anaerobic microbial communities. Environmental Microbiology 8, 371-382. 10.1111/j.1462-2920.2006.00989.x

Stolz, J.F., Basu, P., Santini, J.M., Oremland, R.S., 2006. Arsenic and Selenium in Microbial Metabolism. Annual Review of Microbiology 60, 107-130. 10.1146/annurev.micro.60.080805.142053

Suzuoki, T., 1964. A geochemical study of selenium in volcanic exhalation and sulfur deposits. Bulletin of the Chemical Society of Japan 37, 1200-1206.

Tan, T., Beydoun, D., Amal, R., 2003a. Effects of organic hole scavengers on the photocatalytic reduction of selenium anions. Journal of Photochemistry and Photobiology A: Chemistry 159, 273-280. 10.1016/S1010-6030(03)00171-0

Tan, T., Beydoun, D., Amal, R., 2003b. Photocatalytic reduction of Se(VI) in aqueous solutions in UV/TiO_2 system: importance of optimum ratio of reactants on TiO2 surface. Journal of Molecular Catalysis A: Chemical 202, 73-85. 10.1016/S1381-1169(03)00205-X

Tan, T., Beydoun, D., Amal, R., 2003c. Photocatalytic Reduction of Se(VI) in Aqueous Solutions in UV/TiO_2 System: Kinetic Modeling and Reaction Mechanism. Journal of Physical Chemistry B 107, 4296-4303. 10.1021/jp026149+

Taratus, E.M., S.G. Eubanks, T.J. DiChristina, 2000. Design and application of a rapid screening technique for isolation of selenite reduction-deficient mutants of *Shewanella putrefaciens*. Microbiological Research 155, 79-85.

Taylor, S.R., 1964. Abundance of chemical elements in the continental crust: a new table. Geochimica et Cosmochimica Acta 28, 1273-1285. 10.1016/0016-7037(64)90129-2

Thickpenny, A., 1984. The sedimentology of the Swedish Alum Shales. Geological Society, London, Special Publications 15, 511-525. 10.1144/gsl.sp.1984.015.01.33

Tokunaga, T.K., Lipton, D.S., Benson, S.M., Yee, A.W., Oldfather, J.M., Duckart, E.C., Johannis, P.W., Halvorsen, K.E., 1991. Soil selenium fractionation, depth profiles and time trends in a vegetated site at Kesterson Reservoir. Water, Air, & Soil Pollution 57-58, 31-41. 10.1007/BF00282866

Tomei, F.A., Barton, L.L., Lemanski, C.L., Zocco, T.G., Fink, N.H., Sillerud, L.O., 1995. Transformation of Selenate and Selenite to Elemental Selenium by Desulfovibrio-Desulfuricans. Journal of Industrial Microbiology 14, 329-336. 10.1007/BF01569947

Tudge, A.P., Thode, H.G., 1950. Thermodynamic Properties of Isotopic Compounds of Sulfur. Canadian Journal of Research Sec. B 28, 567-578.

Turekian, K.K.a.W., K.H., 1961. Distribution of the Elements in Some Major Units of the Earth's Crust. Geological Society of America Bulletin 72, 175-192.

Turgeon, S.C., Creaser, R.A., 2008. Cretaceous oceanic anoxic event 2 triggered by a massive magmatic episode. Nature 454, 323-326. 10.1038/nature07076

Tyson, R.V., 1987. The genesis and palynofacies characteristics of marine petroleum source rocks. Geological Society, London, Special Publications 26, 47-67. 10.1144/gsl.sp.1987.026.01.03

Tyson, R.V., Pearson, T.H., 1991. Modern and ancient continental shelf anoxia: an overview. Geological Society, London, Special Publications 58, 1-24. 10.1144/gsl.sp.1991.058.01.01

Van Cappellen, P., Ingall, E.D., 1994. Benthic Phosphorus Regeneration, Net Primary Production, and Ocean Anoxia: A Model of the Coupled Marine Biogeochemical Cycles of Carbon and Phosphorus. Paleoceanography 9, 677-692. 10.1029/94pa01455

Van Cappellen, P., Ingall, E.D., 1996. Redox stabilization of the atmosphere and oceans by phosphorus-limited marine productivity. Science 271, 493-496.

van der Weijden, C.H., Reichart, G.J., van Os, B.J.H., 2006. Sedimentary trace element records over the last 200 kyr from within and below the northern Arabian Sea oxygen minimum zone. Marine Geology 231, 69-88. DOI: 10.1016/j.margeo.2006.05.013

Vandermeulen, J.H., Foda, A., 1988. Cycling of selenite and selenate in marine phytoplankton. Marine Biology 98, 115-123.

Weiss, H.V., Koide, M., Goldberg, E.D., 1971. Selenium and Sulfur in a Greenland Ice Sheet: Relation to Fossil Fuel Combustion. Science 172, 261-263. 10.1126/science.172.3980.261

Wen, H., Carignan, J., 2007. Reviews on atmospheric selenium: Emissions, speciation and fate. Atmospheric Environment 41, 7151-7165. 10.1016/j.atmosenv.2007.07.035

Wen, H., Carignan, J., 2011. Selenium isotopes trace the source and redox processes in the black shale-hosted Se-rich deposits in China. Geochimica et Cosmochimica Acta 75, 1411-1427. DOI: 10.1016/j.gca.2010.12.021

Wen, H., Carignan, J., Hu, R., Fan, H., Chang, B., Yang, G., 2007. Large selenium isotopic variations and its implication in the Yutangba Se deposit, Hubei Province, China. Chinese Science Bulletin 52, 2443-2447.

Wignall, P.B., 1994. Black Shales. Oxford University Press, Oxford.

Woolfolk, C.A., Whiteley, H.R., 1962. Reduction of Inorganic Compounds with Molecular hydrogen by

Micrococcus lactulyticus I.: Stoichiometry with Compounds of Arsenic, Selenium, Tellurium, Transition and Other Elements. J. Bacteriol. 84, 647-658.

Wrench, J.J., Measures, C.I., 1982. Temporal variations in dissolved selenium in a coastal ecosystem. Nature 299, 431-433.

Xu, X.-M., Carlson, B., Zhang, Y., Mix, H., Kryukov, G., Glass, R., Berry, M., Gladyshev, V., Hatfield, D., 2007. New Developments in Selenium Biochemistry: Selenocysteine Biosynthesis in Eukaryotes and Archaea. Biological Trace Element Research 119, 234-241. 10.1007/s12011-007-8003-9

Yu, M., Tian, W., Sun, D., Shen, W., Wang, G., Xu, N., 2001. Systematic studies on adsorption of 11 trace heavy metals on thiol cotton fiber. Analytica Chimica Acta 428, 209-218. 10.1016/S0003-2670(00)01238-1

Zawislanski, P.T., McGrath, A.E., 1998. Selenium Cycle in Estuarine Wetlands: Overview and New Results from the San Francisco Bay, in: Frankenberger Jr., W.T., Engberg, R.A. (Ed.), Environmental Chemistry of Selenium. Marcel Dekker, INC., New York, pp. 223-242.

Zehr, J.P., Oremland, R.S., 1987. Reduction of Selenate to Selenide by Sulfate-Respiring Bacteria: Experiments with Cell Suspensions and Estuarine Sediments. Applied and Environmental Microbiology 53, 1365-1369.

Zhang, Y., Moore, J.N., 1996. Selenium Fractionation and Speciation in a Wetland System. Environmental Science & Technology 30, 2613-2619. 10.1021/es960046l

Zhang, Y., Zahir, Z.A., Frankenberger, W.T., Jr., 2004. Fate of Colloidal-Particulate Elemental Selenium in Aquatic Systems. J Environ Qual 33, 559-564.

Zhu, J.-M., Johnson, T.M., Clark, S.K., Zhu, X.-K., 2008. High Precision Measurement of Selenium Isotopic Composition by Hydride Generation Multiple Collector Inductively Coupled Plasma Mass Spectrometry with a ^{74}Se-^{77}Se Double Spike. Chinese Journal of Analytical Chemistry 36, 1385-1390. 10.1016/S1872-2040(08)60075-4